AD-A110 604 NAVAL POSTGRADUATE SCHOOL MONTEREY CA F/G 21/5
THE BI-PHASE NOZZLE.(U)
SEP 81 N E FLENNIKEN
UNCLASSIFIED NL

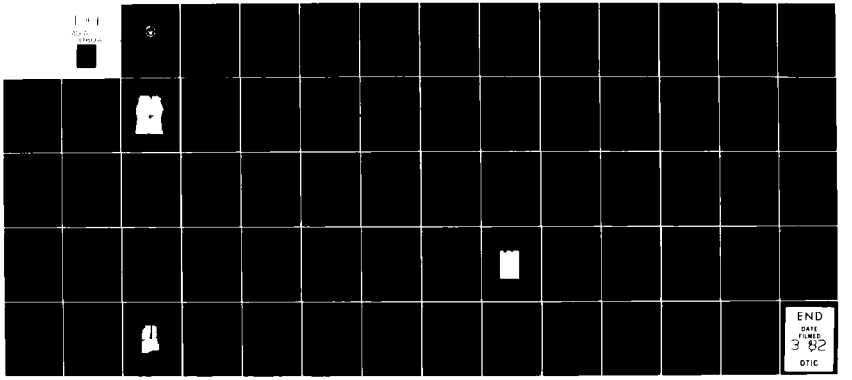

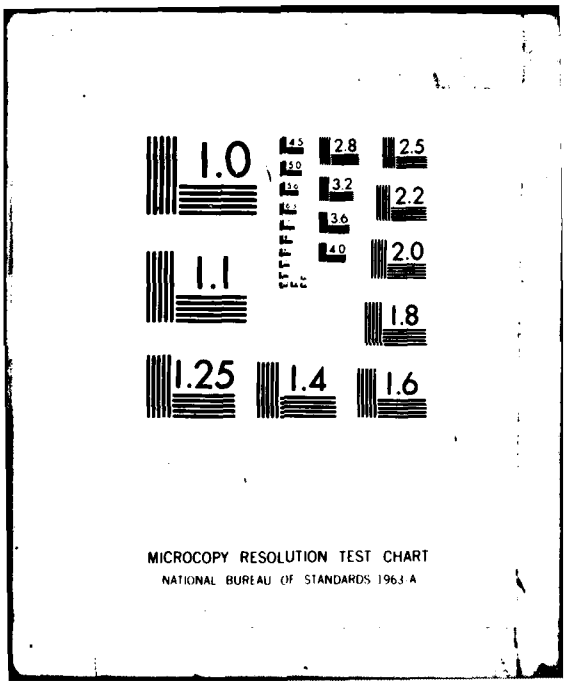
1.0
1.1
1.25
1.4
1.6
1.8
2.0
2.2
2.5
2.8
3.2
3.6
4.0
4.5
5.0
5.6
MICROCOPY RESOLUTION TEST CHART
NATIONAL BUREAU OF STANDARDS 1963 A

LEVEL II

NAVAL POSTGRADUATE SCHOOL
Monterey, California

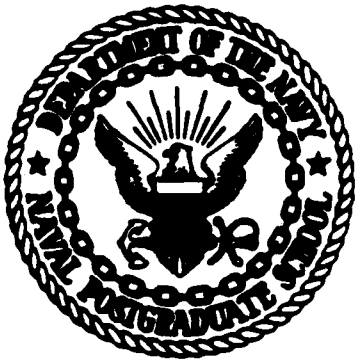

THESIS

THE BI-PHASE NOZZLE

by

Michael E. Flenniken

September 1981

Thesis Advisor: Joseph Sladky

Approved for public release; distribution unlimited

UNCLASSIFIED

SECURITY CLASSIFICATION OF THIS PAGE (When Data Entered)

REPORT DOCUMENTATION PAGE	READ INSTRUCTIONS BEFORE COMPLETING FORM
1. REPORT NUMBER	2. GOVT ACCESSION NO. AD-A110604	3. RECIPIENT'S CATALOG NUMBER
4. TITLE (and Subtitle) The Bi-phase Nozzle	5. TYPE OF REPORT & PERIOD COVERED Master's Thesis September 1981
	6. PERFORMING ORG. REPORT NUMBER
7. AUTHOR(s) Michael E. Flenniken	8. CONTRACT OR GRANT NUMBER(s)
9. PERFORMING ORGANIZATION NAME AND ADDRESS Naval Postgraduate School Monterey, California 93940	10. PROGRAM ELEMENT, PROJECT, TASK AREA & WORK UNIT NUMBERS
11. CONTROLLING OFFICE NAME AND ADDRESS Naval Postgraduate School Monterey, California 93940	12. REPORT DATE September 1981
	13. NUMBER OF PAGES 66 pages
14. MONITORING AGENCY NAME & ADDRESS(if different from Controlling Office)	15. SECURITY CLASS. (of this report) Unclassified
	15a. DECLASSIFICATION/DOWNGRADING SCHEDULE

16. DISTRIBUTION STATEMENT (of this Report)

Approved for public release; distribution unlimited.

17. DISTRIBUTION STATEMENT (of the abstract entered in Block 20, if different from Report)

18. SUPPLEMENTARY NOTES

19. KEY WORDS (Continue on reverse side if necessary and identify by block number)

Nozzle, Bi-phase, Two-phase, Bi-phase cycle thermodynamics.

20. ABSTRACT (Continue on reverse side if necessary and identify by block number)

The purpose of this effort was to gain an insight into the Bi-phase cycle concept and to develop an experimental facility to test the key component of this power cycle--the Bi-phase nozzle. A system was developed and checked out that allows testing different Bi-phase nozzle shapes. The experimental system is provided with sufficient instrumentation to allow for the determination of the nozzle performance. In addition to the standard gas and liquid flow rates, measurement provisions exist for survey of the

DD FORM 1 JAN 73 1473 EDITION OF 1 NOV 65 IS OBSOLETE S/N 0102-014-6601

UNCLASSIFIED

SECURITY CLASSIFICATION OF THIS PAGE (When Data Entered)

nozzle exit plane. Measurements can be made for the gas/liquid ratio and velocities at the nozzle exit.

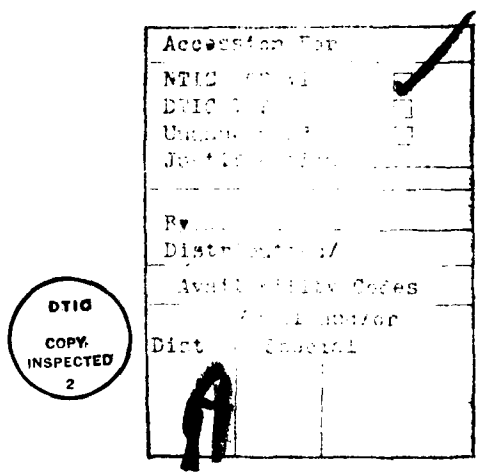

Approved for public release; distribution unlimited

The Bi-phase Nozzle

by

Michael E. Flenniken
Lieutenant Commander, United States Navy
B.S., University of Nebraska, 1971

Submitted in partial fulfillment of the
requirements for the degree of

MASTER OF SCIENCE IN MECHANICAL ENGINEERING

from the

NAVAL POSTGRADUATE SCHOOL
September 1981

Author Michael E. Flenniken

Approved by: J. Gordon Leishman
Thesis Advisor

David Salinas
Second Reader

for R. E. Newton
Chairman, Department of Mechanical Engineering

William M. Tolles
Dean of Science and Engineering

ABSTRACT

The purpose of this effort was to gain an insight into the Bi-phase cycle concept and to develop an experimental facility to test the key component of this power cycle--the Bi-phase nozzle. A system was developed and checked out that allows testing different Bi-phase nozzle shapes. The experimental system is provided with sufficient instrumentation to allow for the determination of the nozzle performance. In addition to the standard gas and liquid flow rates, measurement provisions exist for survey of the nozzle exit plane. Measurements can be made for the gas/liquid ratio and velocities at the nozzle exit.

TABLE OF CONTENTS

LIST OF FIGURES

ACKNOWLEDGMENT

I wish to express my appreciation to Professor Sladky for his invaluable aid in completing this project, to my wife, Joyce, for her exemplary typing skills and patience, and finally to Dr. Roger Husted who provided the necessary "vision."

I. INTRODUCTION

Low speed prime mover systems in marine applications are attractive in that they negate requirements for heavy, voluminous and noisy reduction gearing. Direct drive conventional steam turbines and conventional electric drives have been tested and utilized with only limited success. What is required is a machine with low specific speed that is compatible at the same time with existing heat source systems. One option that may meet these requirements is the Bi-phase prime mover. The Bi-phase turbine is a machine having low specific speed and high torque. As such, it is ideally suited for marine propulsion. The Bi-phase turbine can drive the propellers directly without gear reduction. This feature leads to improvements in weight, volume and noise reduction.

In addition, certain aspects of the Bi-phase concept may allow increased power production efficiencies. It may be possible to achieve near constant temperature expansion in the two-phase nozzle thus realizing a degree of "Carnotization" of the basic Rankine cycle. A detailed description of the Bi-phase power plant is given in Section III.

A key element in the development of the Bi-phase prime mover is the Bi-phase nozzle. A Bi-phase nozzle is a flow accelerator in which fluid particles or droplets are

accelerated by a vapor. The liquid and vapor may be chemically identical or dissimilar. The expanding vapor imparts kinetic energy to the liquid droplets. During this expansion, the droplets may also transfer heat to or from the vapor, resulting in a near isothermal expansion. In the nozzle, most of the available thermal energy of the vapor is converted to kinetic energy of the liquid droplets. The nozzle is converging-diverging, a requirement resulting from the low sonic velocity in two-phase mixtures. Computer codes [Ref. 1] exist that yield nozzle exit velocities to reasonable accuracies provided fluid properties are known, liquid particle size can be controlled, and one dimensionally in the flow field is assumed.

Tangren, Dodge, and Siefert derived the equations for isentropic flow of an immiscible two-component mixture with equal temperatures of the liquid and the gas. The first extensive experiments on two-phase nozzles were performed by Elliott [Ref. 1].

The purpose of this effort is to develop an experimental facility that will allow evaluation of two-phase nozzle concepts and associated liquid-vapor interaction phenomenon. The ultimate goal is to provide experimental capability to validate analytic models of Bi-phase nozzles. To this end an experimental system was designed that includes a high degree of flexibility to allow for rapid flow passage

geometry variation. The instrumentation installed has the capability to sample liquid content at different points in the nozzle exit plane.

II. BACKGROUND

Turbine type prime movers, whether based on the Rankine or Brayton cycles, have many advantages. Among these are: high torque at low speed, low vibration levels as compared to internal combustion energy converters, and in some cases very high power densities. Practical considerations result in prime mover power outputs which are at relatively high rotational speeds.

Power demand devices such as propellers and pump jets have rotational speed requirements set by considerations considerably different than those of the prime mover. Unfortunately the rotational speeds of prime mover and power user seldom match. As a consequence, a power conditioning device, a gear box or reduction gearing is invariably mandated. In certain installations the reduction gearing may weigh more than the prime mover.

From a purely thermodynamic consideration one would want the maximum cycle temperature to be as high as possible. However, where the working substance must be contained by physical structures such as combustors, boilers, nozzles, and turbine blades, the cycle temperature limit is set by material considerations. Furthermore, secondary aspects of a prime mover, i.e., safety, may further restrict the range of cycle parameters. A case in

point is the Navy nuclear power plant that does not admit superheat. The turbine inlet conditions are those of saturated vapor. This constrains the maximum cycle efficiency to comparatively low values.

A relatively new prime mover concept that may have the capability to circumvent some of the above identified difficulties is the Bi-phase prime mover. The technology base for the Bi-phase concept is founded in earlier work at the Jet Propulsion Laboratory on liquid metal power generating concepts.

The baseline Bi-phase concept is still the Rankine cycle (Fig. 1). The differences are subtle but of extreme importance. The working fluid is vaporized in the heat addition component of the cycle. This may be a conventional boiler generating high temperature and pressure steam. Normally the working fluid would then enter a nozzle/turbine system and energy would be converted to a mechanical form. In the Bi-phase system, however, a second fluid is introduced at boiler temperature and pressure just prior to the point where the steam enters the nozzles. This second fluid may have a vaporization temperature higher than water and thus will remain in the liquid state throughout the cycle. In the nozzle proper the vapor constituent accelerates and in so doing drags the droplets of the liquid phase to higher velocity (Fig. 2). This energy exchange of enthalpy drop of the vapor to kinetic energy of the liquid is the major departure from the conventional steam power plant.

BI-PHASE CYCLE

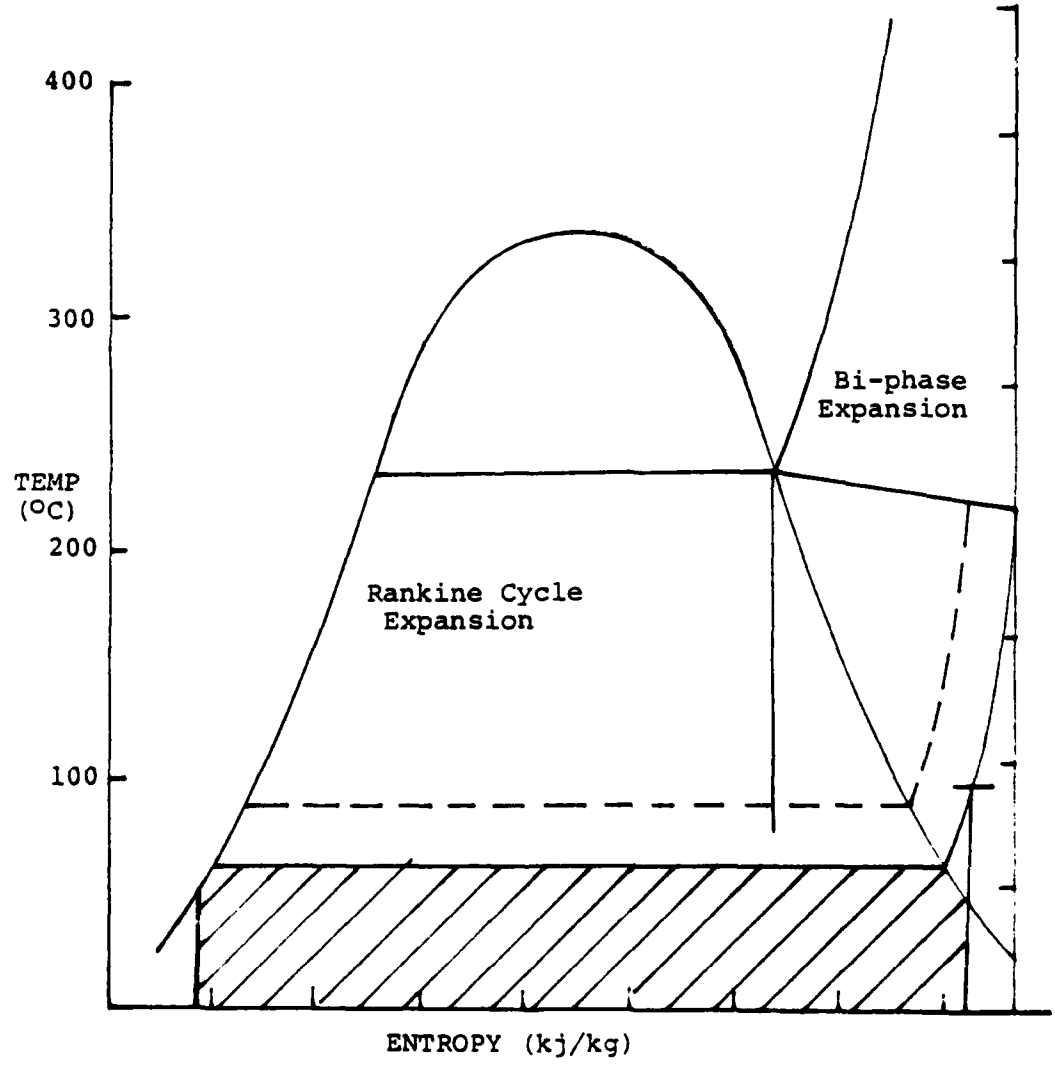

Fig. 1. Temperature-Entropy Diagram

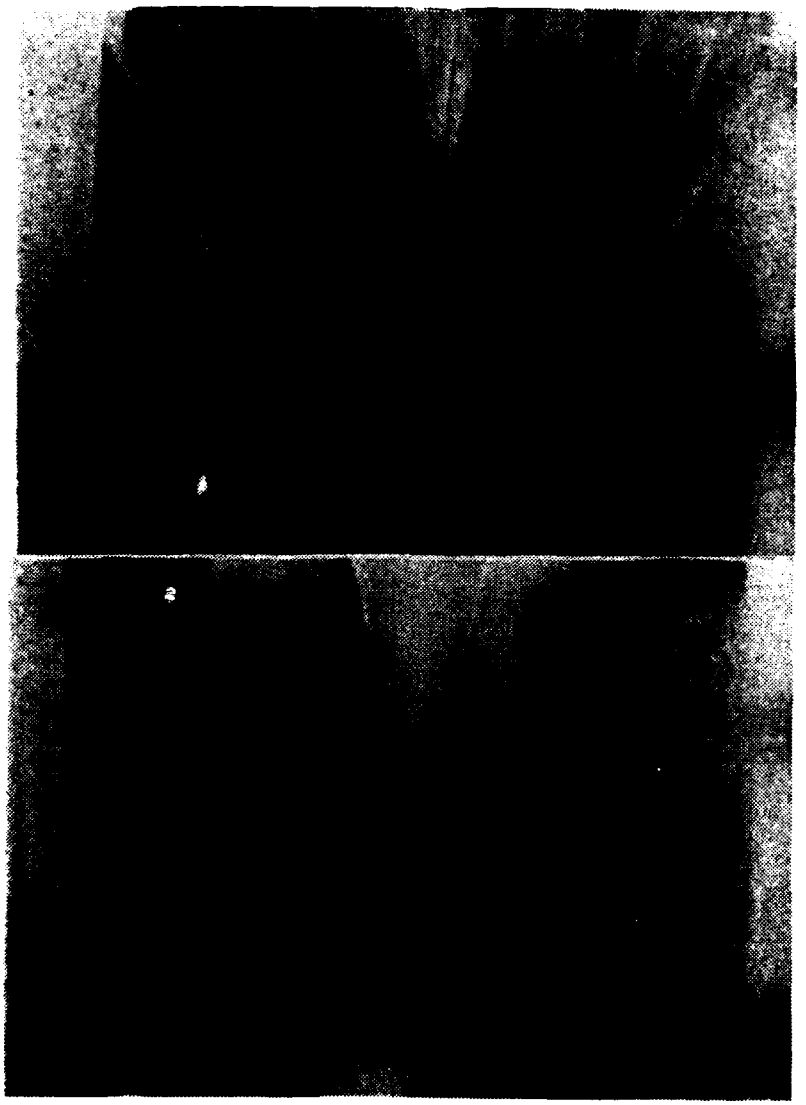

Fig. 2. Liquid Entrainment Photograph

Downstream of the nozzle the high kinetic energy liquid and the expanded vapor are separated. The vapor is condensed and returned to the boiler. The liquid is "parked" on a rotating wheel and energy is extracted by an impulse or pitot type turbine. After interaction with the hydraulic turbine, the fluid is returned for injection at the Bi-phase nozzle mixing section.

It is the Bi-phase aspect of the system that is at the base of some of the potential advantages of the concept, which are:

1. The energy imparted to the liquid phase is in a kinetic form of a high density mass. Hence, the liquid velocities involved are relatively low as compared to velocities of the vapor. Thus the output of the impulse hydraulic turbine will be at high torque and low rotational speeds--more in keeping with rotational speeds of driver elements.
2. The energy extraction from the steam and the energy addition to the liquid takes place in an inherently small device--the Bi-phase nozzle. Thus, the high temperature, pressure, and velocities are confined to a high energy density component.
3. Perhaps the most important aspect is the phenomenon that takes place in the nozzle proper between the liquid and vapor and how this interaction impacts the overall cycle performance. While it is normal

practice to assume "isentropic" expansion in a nozzle, it is not likely that this is what happens in a Bi-phase expansion. In all probability thermal energy is exchanged between the liquid and vapor constituents. This, in fact, may be the most attractive aspect of the Bi-phase concept. If thermal energy can be added to the vapor phase from the liquid, then the expansion can be made to approach an "isothermal" process. The net result is a degree of "Carnotization" of the basic Rankine cycle that can only lead to increased overall cycle efficiencies.

Application of two-phase turbines to Navy propulsion has been examined in two design studies, References 2 and 3. In both cases, the following potential advantages were found when the Bi-phase turbine was compared to advanced steam turbine systems.

1. High efficiency--Full load output power performance gains ranging from 20 to 50 percent were found.
2. Direct drive--Direct drive at speeds ranging from 90-4500 rpm was found possible with a single-stage turbine.
3. Reduced volume--Volume reductions of 30 percent were estimated.
4. High part-load efficiency--Variable mass ratio enabled part-load (cruise) efficiency gains of as much as 100 percent.

An independent Navy study of a large Bi-phase marine turbine arrived at these same conclusions. These potential advantages lead to many possible applications for marine use. Most prominent among these advantages are those applications where space and weight are the most important considerations, for example, torpedoes, submarines, SES, SWATH, etc.

It is thus apparent that the key element of a Bi-phase power system is the Bi-phase nozzle. It is this component that is the subject of this thesis. Specifically, the goal is to develop a research capability to study the flowfield and energy interaction in a Bi-phase nozzle.

III. BI-PHASE CYCLE THERMODYNAMICS

The Bi-phase cycle is basically a variation of the conventional Rankine steam plant. In reality, the "Bi-phase aspect" should be a multicomponent cycle as there is no requirement that the components (vapor and liquid) of the working substance be chemically identical.

In a conventional Rankine cycle (Fig. 1) the liquid phase is introduced to the heat additive component of the system at the maximum cycle pressure. Energy is added and the substance is vaporized. This is a constant pressure energy addition process and follows a constant pressure line on the T-S coordinate system. The maximum cycle temperature may be well into the superheat region. Expansion, often idealized as isentropic, follows. During this pressure drop from boiler to condenser pressures, work is extracted by a turbine via a volume expansion. Constant pressure heat rejection returns the working substance to a liquid phase which then is pumped up to boiler pressure and reintroduced to the heat addition component.

A common way of depicting the maximum cycle efficiency for any cycle is to apply the Carnot efficiency criteria. This Carnot efficiency depends only on temperatures of heat addition and heat rejection.

$$\eta_n = 1 - \frac{Tc}{T_B}$$

Where η_n = Carnot efficiency

T_C = Condenser temperature (^oK)

T_B = Boiler temperature (^oK)

Thus, a cycle operating between source-sink temperatures of 232°C and 64°C respectively has a maximum energy conversion of 33%. The efficiency for a Rankine cycle with the same temperature limits and saturated vapor turbine inlet conditions yields an ideal efficiency of 29%. This efficiency is based strictly on thermodynamic considerations and does not consider irreversibilities such as friction losses, temperature drops in heat exchangers, and hydrodynamic losses in the cycle mechanical components. Furthermore, from practical considerations, the last stages of the expander see a very wet working fluid = 75% quality. This results in erosion and impact losses leading to further decrease in the power generator effectiveness.

It is the Bi-phase cycle variation that has the potential to circumvent the above identified difficulties of the Rankine plant.

The Bi-phase cycle adhieves improved efficiencies because the process involved allows the development of a near Carnot cycle. Thus, the Bi-phase concept achieves a degree of Carnotization of the Rankine cycle. This Carnotization takes place in the Bi-phase nozzle process. While in a

Rankine plant the expansion process is idealized as isentropic; in the Bi-phase system, it can be caused to approach an isothermal process.

There are basically two Bi-phase techniques whereby a Rankine cycle can be caused to approach the Carnot cycle.

A. TWO COMPONENT SYSTEM

One method to Carnotize a steam cycle is to add a second, chemically different component that remains a liquid throughout the cycle process. This component provides a source of heat for the expanding vapor producing a near-isothermal expansion. In Fig. 1 it can be seen that the temperature at the end of the nozzle expansion is 218°C compared to 64°C which would occur in the Rankine cycle. This results in a cycle efficiency of 31% versus 29% for the Rankine cycle. This cycle was invented by D. G. Elliott of Cal Tech for liquid metal MHD. [Ref. 1]

The two-component cycle uses a low vapor pressure liquid and a high vapor pressure liquid having different chemical makeup. Some fluid combinations which have been considered are steam-Krytox, steam-Caloria, steam-lead bismuth eutectic, and Dow-therm-Therminol. The basic advantages of a two-component engine are low rpm, high efficiency with no steam extraction and a more compact turbine. Disadvantages include larger heat exchangers and the complexity of handling two fluids. Figs. 3 and 4 depict two possible methods of utilizing the two-component approach.

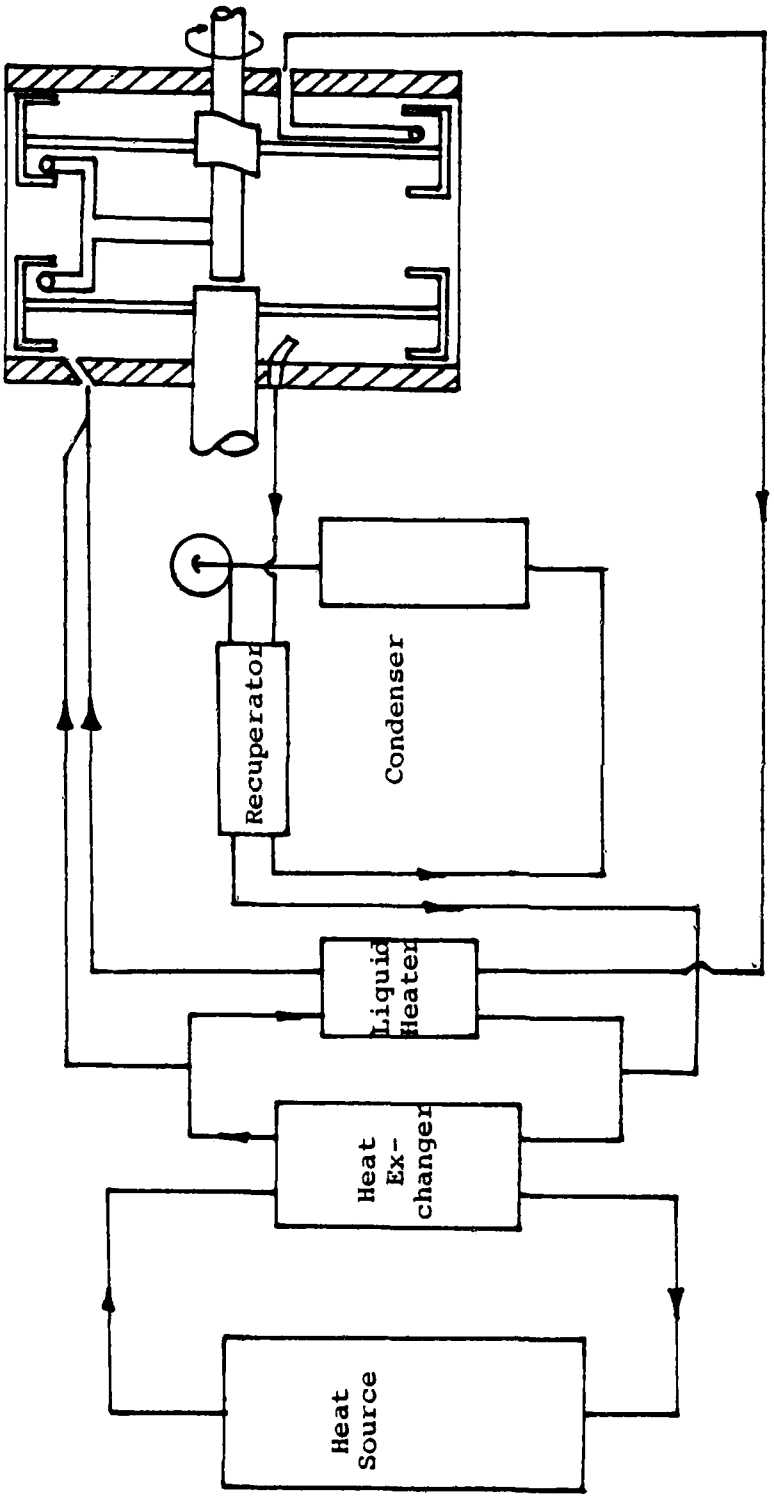

Fig. 3. U-Tube Turbine Engine

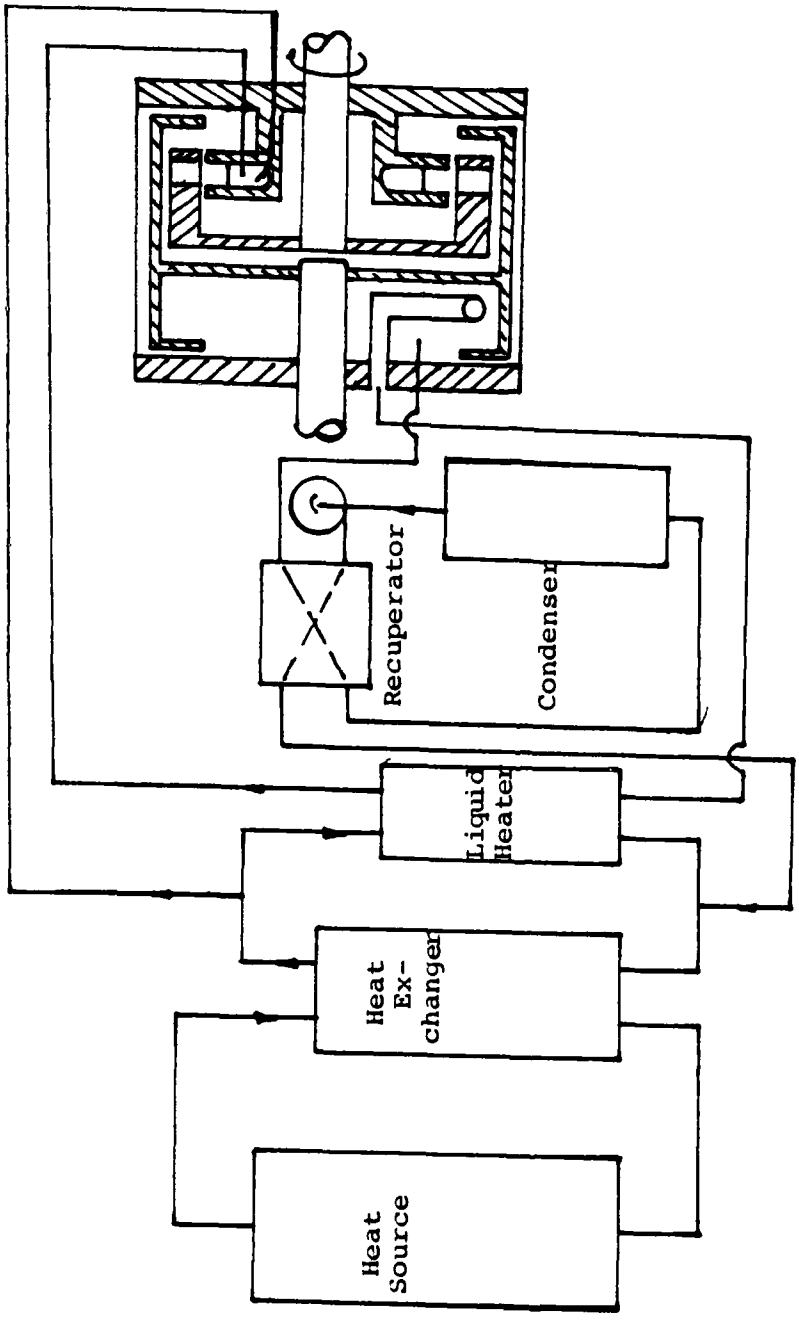

Fig. 4. Impulse Turbine Engine

D. SINGLE COMPONENT SYSTEM

In this cycle the expansion process is ideally paralled to the saturated liquid line that outlines the left hand side of the enthalpy dome. In order to achieve this type of Carnotizing, heat has to be removed during expansion. While it may be possible to do that through the walls of the nozzle, a more conventional way is to extract steam in steps. That means that a scheme of pressure staging is required, where after each expansion stage steam is extracted and used to preheat feed water by condensing all of the extracted steam.

The single component system has the advantage of eliminating oil or heat transfer fluid as the second component. The two-phase mixture in this case consists of steam and water. Typical volume ratios of water to steam are 10:1 or less so this cycle produces somewhat higher values of turbine speed.

In order to obtain high efficiency several expansion stages are used. The five stage system resulting in the temperature-entropy variation of Fig. 5 is shown schematically in Fig. 6. Steam from the heat exchanger flows to the first stage nozzle. A portion of the steam is also used to heat the water flowing to the first stage nozzle. The mixture of primary steam and water is expanded in the nozzle from an inlet vapor quality of 15% to an exit quality of 18%. The two-phase mixture drives a rotary

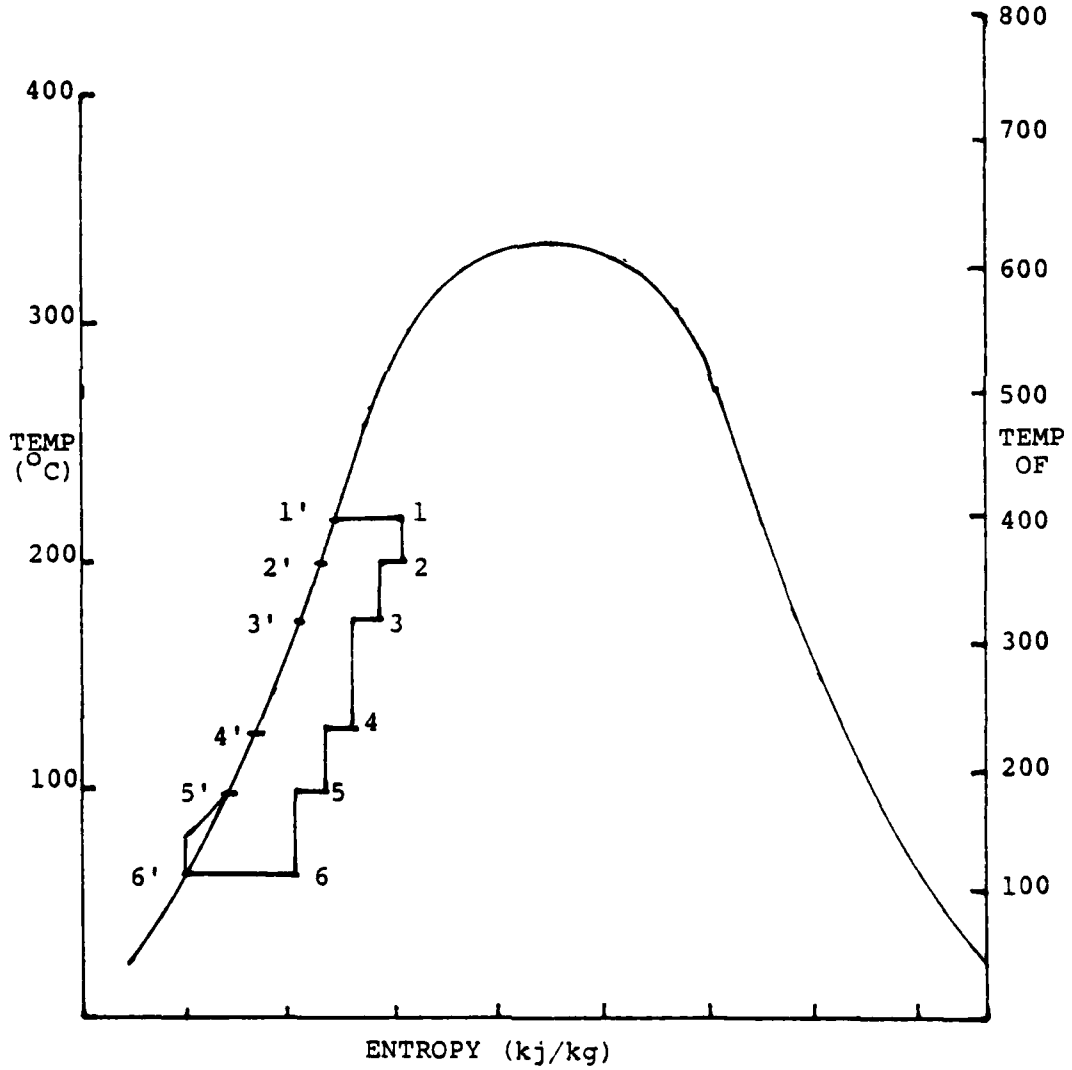

Fig. 5. Single Component Bi-phase Cycle

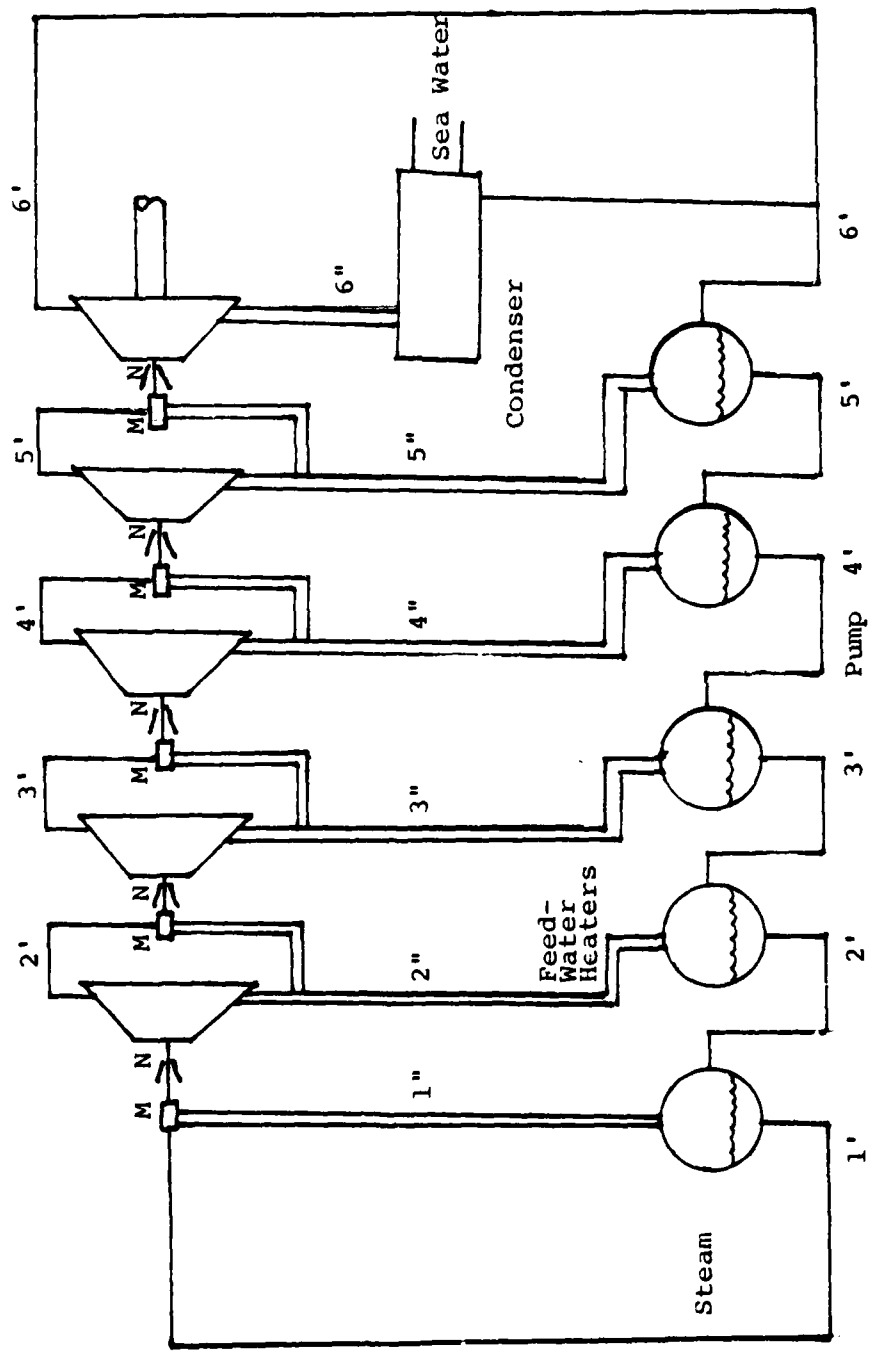

Fig. 6. Wet Steam Five Stage Regenerative Turbine Engine

separator turbine. Part of the separated steam is extracted and flows to a feed water heater. The remainder of the steam is remixed with the water exiting the first stage turbine. This mixture is expanded in the second stage nozzle from an inlet vapor quality of 12% to an exit quality of 18%.

The two-phase mixture drives the second stage rotary separator turbine, where additional steam extraction occurs. In the final stage, steam exhausting from the turbine flows to the condenser. The condensate is remixed with the liquid exiting the last stage turbine. The feed water flows through several stages of a feed water heater where the extraction steam is condensed on the feed water.

Five stages are shown in Fig. 6. The actual number of stages will be determined by a tradeoff between efficiency and cost and complexity.

IV. BI-PHASE NOZZLE THEORY

The Bi-phase nozzle is the key element in the Bi-phase engine concept. While initially it may appear that the design of the nozzle profile is quite straight forward, closer examination will reveal that the question is considerably more complex. The complexity steams from the nature of the working fluid itself. It is a mixture of liquid particles and a compressible gas or vapor.

The complicating factors can be grouped into three categories:

1. The working fluid has two constituents significantly different in density. Thus, there is an aerodynamic interaction between the components (liquid droplets are accelerated by the vapor).
2. The shape and size of the liquid particles is governed by the forces on them. In this particular case the surface tension and inertia forces are of key interest.
3. Thermal interaction between the working fluid components can range from none at all to phase change of the liquid to its vapor form.

Another factor of interest in Bi-phase flow is the question of the velocity of propagation of a disturbance, i.e., velocity of sound. While the velocity in a particular

vapor and in a particular liquid are well established, the situation in a mixture of vapor and liquid is considerably different.

Consider the following discussion from Olson [Ref. 4]. The acoustic velocity in any medium is $c = \sqrt{K/\rho}$, where K is the modulus of elasticity for the medium and ρ is the density. For gas-liquid mixtures the acoustic velocity becomes less than that for either the liquid or gas alone. For a liquid with a small concentration of gas nuclei, the elastic modulus of the mixture is reduced, with no appreciable reduction in density, and thus the acoustic velocity is reduced. For a gas with minute liquid droplets, the density of the mixture is increased with no appreciable change in elastic modulus, and again the acoustic velocity for the mixture is reduced. The velocity of sound in a 14 percent water and 86 percent air mixture is about 30 m/s (depending on the pressure, temperature, and impressed frequency) as compared with about 1460 m/s for water and about 335 m/s for air.

The flow phenomenon of a Bi-phase mixture has been analyzed in Ref. 1. It is repeated as follows. The problem is illustrated in Fig. 7. A spatially uniform two-component mixture of liquid drops and gas enters a nozzle at high pressure and low velocity and expands to low pressure and high velocity. The objective of the analysis is to determine, for a specified pressure, the drop diameter

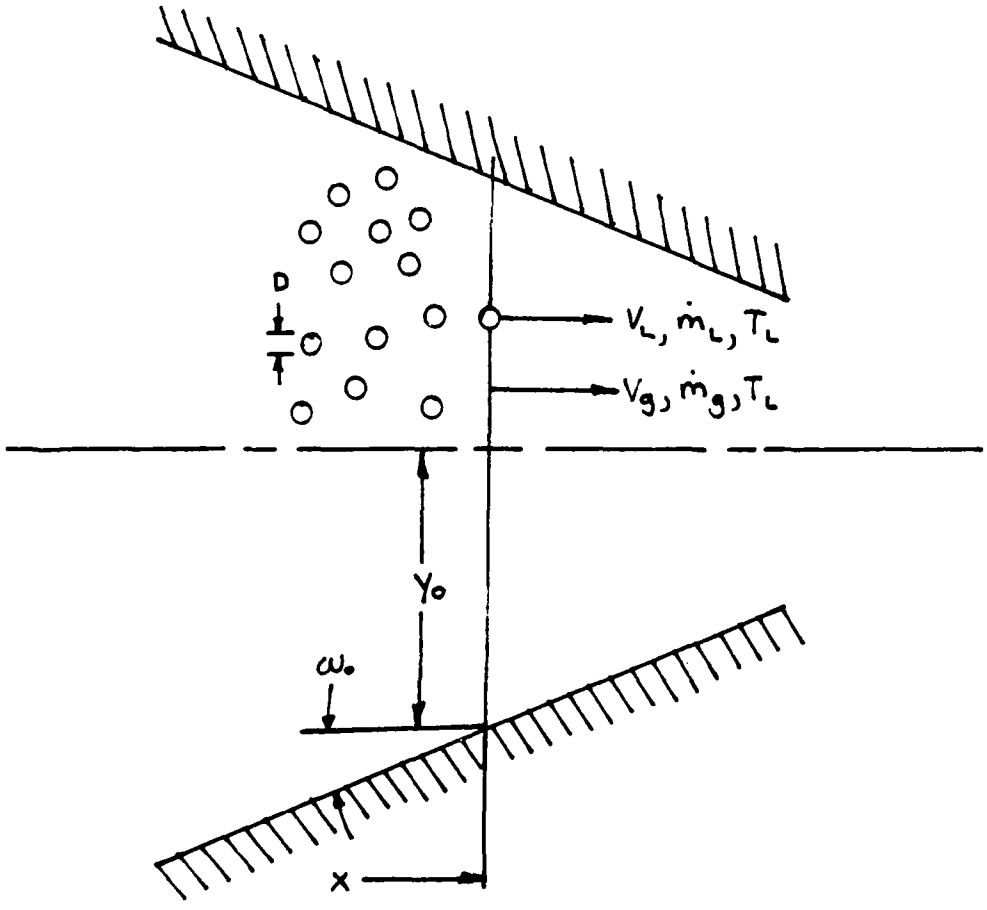

Fig. 7. Two Phase Nozzle Flow and Nomenclature.

D and the temperatures T_g and T_L, velocities V_g and V_L and flow rates $\dot{m}_g$ and $\dot{m}_L$ of the gas and liquid phases, respectively, at each station in the nozzle given the initial values of D, T_g, T_L, V_g, V_L, the total flow rate, and the properties of the fluids.

The five relations employed to compute the five unknowns D, T_g, T_L, V_g, and V_L, are (1) the momentum equation for the mixture, (2) the energy equation for the mixture, (3) the drop drag equation, (4) the drop heat transfer equation, and (5) the drop breakup criterion. Solubility and vapor pressure relations provide the flow rate ratio $\dot{m}_g/\dot{m}_L$.

A. ASSUMPTIONS

The assumptions employed in the two-component analysis are as follows:

1. The liquid is uniformly dispersed as spherical drops all of the same diameter.
2. The drops break up to limit the Weber number to 6.
3. There are no external forces acting on the two-phase mixture other than pressure and wall shear, and there is no heat transfer to or from the mixture.
4. The flow is one-dimensional.
5. The drops are large enough for the surface curvature to have negligible effect on the vapor pressure of the liquid and for the surface energy to be negligible.
6. The drops are isothermal.
7. The gas mixture obeys the additive-pressure law.

8. The partial pressure of the predominantly liquid component in the liquid is given by Raoult's Law.
9. The concentration of the predominantly gaseous component in the liquid is given by Henry's Law.
10. The volume of the liquid solution is equal to the sum of the volumes of the pure liquids.

Assumption 1 restricts the analysis to nozzles having spatially uniform injection of the liquid into the gas and operating at gas-to-liquid volume ratios greater than unity. Assumption 2, the drop breakup criterion, states that drop diameter is limited to a value D for which W_e $W_e = \rho_g V_g^2 D/2\sigma = 6$. Thus

$$D_{max} = \frac{12\sigma}{\rho_g V_g^2} \tag{1}$$

where ρ_g is the gas density, V_s is the slip velocity $V_g - V_L$, and σ is the liquid surface tension. The form of Eq. (1) is physically reasonable in that the Weber number is proportional to the ratio of stagnation pressure $\rho_g V_s^2/2$ to surface tension pressure $4\sigma/D$. Hence, a drop would be expected to flatten and break up at a sufficiently high value of We. This has been verified experimentally and the critical Weber number found to be 6, within a factor of about two. An additional restriction is that for actual breakup to occur, the time spent at a Weber number exceeding 6 must be longer than the natural period of oscillation of the drop,

$\pi(\rho_L D^3/\sigma)^{\frac{1}{2}}/4$, where ρ_L is the density of the liquid. This requirement is met only in two-phase nozzles longer than about 10 in. and Assumption 2 may cause the analysis to overestimate the exit velocity by increasing amounts as the nozzle length decreases below 10 in.

Assumption 3 excludes magnetohydrodynamic and mechanical body forces. The exclusion of wall heat transfer is correct for the insulated nozzles of interest for power systems. In addition, the relatively high velocity results in short residence lines in the nozzle proper.

Assumption 4 is closely met in practical nozzles since good performance requires small wall angles, large throat radius of curvature, and uniformly distributed injection of the fluids at the nozzle entrance.

Assumption 5 is valid for the drop sizes of 0.001 to 0.010 in. produced by the Eq. (1) breakup criterion. Assumption 6 is valid because of the rapid internal circulation in drops. Assumption 7 introduces negligible error in most cases of practical interest since the vapor pressure of the liquid is small and needs only to be evaluated approximately.

Assumptions 8, 9, and 10 are either valid, or cause little error, for fluids of low miscibility, which are the fluids of interest.

B. DERIVATION OF EQUATIONS FOR FREE-STREAM FLOW

1. Continuity

Referring to Fig. 1, the nozzle flow area A is equal to the gas flow area $\dot{m}_g/\rho_g V_g$ plus the liquid flow area $\dot{m}_L/\rho_L V_L$. Thus,

$$A = \dot{m}_g \left(\frac{1}{\rho_g V_g} + \frac{r}{\rho_l V_l} \right) \tag{2}$$

where r is the mass mixture ratio $\dot{m}_L/\dot{m}_g$.

2. Momentum

By Assumption 3, the only force acting on the free-stream flow is that due to the pressure gradient. If $\dot{M}$ is the momentum flux at flow area A, the change in momentum flux across pressure increment dp is

$$d\dot{M} = -Adp \tag{3}$$

The momentum flux can be written as the sum of the momentum fluxes of the gas and liquid. Thus,

$$\dot{M} = \dot{m}_g V_g + \dot{m}_l V_l \tag{4}$$

If the flow were allowed to continue at constant pressure, V_g and V_L would become equal to each other at the mass-weighted mean velocity $\bar{V}$. Since for this process, $d\dot{M} = 0$, the value of $\bar{V}$ is given by

$$(\dot{m}_g + \dot{m}_l)\bar{V} = \dot{m}_g V_g + \dot{m}_l V_l \tag{5}$$

or

$$\bar{V} = \frac{V_g + rV_l}{1 + r} \tag{6}$$

Thus, the momentum flux can be written

$$\dot{M} = (\dot{m}_g + \dot{m}_l)\bar{V} \tag{7}$$

Since $\dot{m}_g + \dot{m}_L$ is constant, the change in momentum flux is

$$d\dot{M} = (\dot{m}_g + \dot{m}_l)d\bar{V} \tag{8}$$

Substituting Eqs. (8) and (2) into Eq. (3), $d\bar{V}$ can be written

$$d\bar{V} = \frac{1}{1 + r}\left(\frac{1}{p_g V_g} + \frac{r}{p_l V_l}\right) dp \tag{9}$$

The slip ratio is defined as

$$s = V_g/\bar{V} = (V_g - V_l)/\bar{V} \tag{10}$$

This equation can be combined with Eq. (6) to give V_g and V_L in terms of $\bar{V}$:

$$V_g = \left(1 + \frac{rs}{1 + r}\right)\bar{V} = a\bar{V} \tag{11}$$

$$V_l = \left(1 - \frac{s}{1 + r}\right)\bar{V} = b\bar{V} \tag{12}$$

The gas density can be expressed as

$$p_g = W_g p/RT_g \tag{13}$$

where W_g is the effective molecular weight of the gas mixture and R is the universal gas constant. Eq. (13) is the definition of the effective molecular weight W_g, which is the

quantity that gives the actual gas density when substituted in Eq. (13).

Substituting Eqs. (11)-(13) into Eq. (9), the differential momentum equation is

$$2\bar{V}d\bar{V} = d\bar{V}^2 = - \frac{2}{1 + r}\left(\frac{RT_g}{aW_g p} + \frac{r}{b\rho_l}\right) dp \qquad (14)$$

The quantities a and b are slowly varying because s is typically only 0.1 to 0.3 and slowly varying. The quantities r, T_g, W_g and ρ_L are also slowly varying. Integrating Eq. (14) over a pressure increment Δp, for which a, b, r, T_g, W_g, and ρ_L are constant to within the desired accuracy, the change in V^2 is

$$\Delta\bar{V}^2 = - \int_{p-\frac{\Delta p}{2}}^{p+\frac{\Delta p}{2}} \frac{2}{1 + 4}\left(\frac{RT_g}{aW_g p} + \frac{r}{b\rho_l}\right) dp \qquad (15)$$

All quantities other than pressure can be taken outside the integral and evaluated at their mean values (denoted by subscript m) corresponding to the mid-interval pressure p. Thus,

$$\Delta\bar{V}^2 = - \frac{2}{1 + r_m} \times\left(\frac{RT_{g_m}}{a_m W_{g_m}} \int_{p-\frac{\Delta p}{2}}^{p+\frac{\Delta p}{2}} \frac{dp}{p} + \frac{r_m}{b_m \rho_{l_m}} \int_{p-\frac{\Delta p}{2}}^{p+\frac{\Delta p}{2}} dp\right) \qquad (16)$$

Performing the integrations,

$$\Delta\overline{V^2} = -\frac{2}{1 + r_m}\left(\frac{RT_{g_m}}{a_m W_{g_m}} \log_e \frac{p + \Delta p/2}{p - \Delta p/2} + \frac{r_m \Delta p}{b_m \rho l_m}\right) \quad (17)$$

Equation (17) is the final form of the momentum equation.

3. Energy

The enthalpy change of the mixture between state 1 (the beginning of pressure interval Δp) and state 2 (the end of the interval) can be evaluated in two steps: (1) phase change at p_1, T_{g_1}, T_{L_1} and (2) change to P_2, T_{L_2} T_{g2}, at fixed composition.

The enthalpy change for step 1 is

$$\Delta H_1 = \begin{bmatrix}\text{amount of A} \\ \text{vaporized}\end{bmatrix} \times \begin{bmatrix}\text{enthalpy required} \\ \text{to vaporize and} \\ \text{heat unit mass of} \\ \text{A from } T_L \text{ to } T_{gL}\end{bmatrix}$$

$$+ \begin{bmatrix}\text{amount of B} \\ \text{vaporized}\end{bmatrix} \times \begin{bmatrix}\text{enthalpy required} \\ \text{to vaporize and} \\ \text{heat unit mass of} \\ \text{B from } V_{L_1} \text{ to } T_{g_1}\end{bmatrix}$$

$$+ \begin{bmatrix}\text{amount of A} \\ \text{and B} \\ \text{vaporized}\end{bmatrix} \times \begin{bmatrix}\text{kinetic energy} \\ \text{required to} \\ \text{accelerate unit} \\ \text{mass from } V_{L_1} \text{ to} \\ V_{g_1}\end{bmatrix}$$

or

$$\Delta H_1 = (\dot{m}_{a_{g_2}} - \dot{m}_{a_{g_1}})[L_{a_1} + c_{a_{g_1}}(T_{g_1} - T_{l_1})]$$

$$+ (\dot{m}_{b_{g_2}} - \dot{m}_{b_{g_2}})[L_{b_1} + c_{b_{g_1}}(T_{g_1} - T_{l_1})]$$

$$+ (\dot{m}_{g_2} - \dot{m}_{g_1})(V_{g_1}^2 - V_{l_1}^2)/2 \qquad (18)$$

where L and c are latent heat and specific heat, respectively.

Introducing more compact notation,

$$\Delta H_1 = \Delta\dot{m}_{a_g}(L_{a_1} + c_{a_{g_1}}\delta_1 T)$$

$$+ \Delta m_{b_2}(L_{b_1} + c_{b_{g_1}}\delta_1 T) + \frac{\Delta\dot{m}_g \delta_1 V^2}{2} \qquad (19)$$

The enthalpy change for step 2 is evaluated from the temperature, pressure, and velocity changes, with properties evaluated at mean T and p for the interval.

$$\Delta H_2 = \dot{m}_{g_2}[c_{g_m}(T_{g_2} - T_{g_1}) + \tfrac{1}{2}(V_{g_2}^2 - V_{g_1}^2)]$$

$$+ \dot{m}_{l_2}[c_{l_m}(T_{l_2} - T_{l_1}) + \frac{p_2 - p_1}{p_{l_m}}$$

$$+ \tfrac{1}{2}(V_{l_2}^2 - V_{l_1}^2)] \qquad (20)$$

$$= \dot{m}_{g_2}\left(c_{g_m}\Delta T_g + \frac{\Delta v_g^2}{2}\right)$$

$$+ \dot{m}_{l_2}\left(c_{l_m}\Delta T_l + \frac{\Delta p}{\rho l_m} + \frac{\Delta v_l^2}{2}\right) \qquad (21)$$

By Assumption 3, no work is done by the free-stream flow and no heat is transferred to it. Hence,

$$\Delta H_1 + \Delta H_2 = 0 \qquad (22)$$

Substituting Eqs. (19) and (21) into Eq. (22) and solving for ΔT_g gives the energy equation for the mixture:

$$\Delta T_g = -\frac{1}{c_{g_m}}\left[\frac{\Delta v_g^2}{2} + r_2\left(c_{l_m} T_l + \frac{\Delta p}{\rho l_m} + \frac{\Delta v_l^2}{2}\right)\right.$$

$$+ \frac{\Delta \dot{m}_g \delta_l v^2}{2\dot{m}_{g_2}} + \frac{\Delta \dot{m}_{a_g}}{\dot{m}_{g_2}}\left(L_{a_l} + c_{a_{g_l}}\delta_l T\right)$$

$$\left. + \frac{\Delta m_{b_g}}{\dot{m}_{g_2}}\left(L_{b_l} + c_{b_{g_l}}\delta_l T\right)\right] \qquad (23)$$

4. Drag

Although no force other than pressure acts on the free-stream flow as a whole, a drag force exists between the phases. Hence, a second momentum equation must be written using as the control volume the boundary between the phases.

The two forces acting on each liquid drop are the buoyancy due to the pressure gradient and the drag due to

the relative gas velocity. The sum of these is equal to the mass times the acceleration of the drop. Thus, for a single drop.

$$\begin{bmatrix}\text{dynamic pressure of}\\ \text{relative gas flow}\end{bmatrix} \times \begin{bmatrix}\text{drag co-}\\ \text{efficient}\end{bmatrix} \times \begin{bmatrix}\text{frontal area}\\ \text{of drop}\end{bmatrix} - \begin{bmatrix}\text{volume}\\ \text{of drop}\end{bmatrix} \times \begin{bmatrix}\text{pressure}\\ \text{gradient}\end{bmatrix} = \begin{bmatrix}\text{mass}\\ \text{of drop}\end{bmatrix} \times \begin{bmatrix}\text{accelera-}\\ \text{tion of drop}\end{bmatrix}$$

or

$$\left(\frac{1}{2}\rho_g|V_2|V_2\right) C_D \frac{\pi D^2}{4} - \frac{\pi D^2}{6}\frac{dp}{dx} = \left(\frac{\pi D^3}{6}\rho_L\right)\left(V_1 \frac{dV_1}{dx}\right) \tag{24}$$

The absolute value sign in the first term makes the drag force positive when $V_g > V_L$ and negative when $V_g < V_L$.

Solving Eq. (24) for dV_L,

$$dV_1 = \frac{S\rho_g|s|s\bar{V}^2 C_\rho dx}{4\rho_1 V_1 D} - \frac{dp}{\rho_1 V_1} \tag{25}$$

Differentiating Eq. (12), dV_L can also be expressed in terms of s, r, and $\bar{V}$. Thus,

$$dV_1 = bd\bar{V} + \bar{V}\left[\frac{sdr}{(1+r)^2} - \frac{ds}{1+r}\right] \tag{26}$$

Solving for ds,

$$ds = \frac{b(1+r)d\bar{V}}{\bar{V}} + \frac{sdr}{1+r} - \frac{(1+r)dV_1}{\bar{V}} \tag{27}$$

Substituting dV_L from Eq. (25), noting that $d\bar{V} = d\bar{V}^2/2\bar{V}$, using Eq. (12), and writing for a finite increment, results in,

$$\Delta s = \frac{b_m(1 + r_m)\Delta\bar{V}^2}{2\bar{V}_m^2} + \frac{(1 + r_m)\Delta p}{b_m\rho_{l_m}\bar{V}_m^2} + \frac{s_m\Delta r}{1 + r_m}$$

$$- \frac{3\rho_{g_m}|s_m|s_m C_{D_m}(1 + r_m)\Delta x}{4b_m\rho_{l_m}D} \qquad (28)$$

This is the drag equation employed when x is specified as a function of p.

Solving Eq. (28) for Δx yields the required alternative equation:

$$\Delta x = \frac{4D}{3\rho_{g_m}|s_m|s_m C_{D_m}\bar{V}^2}\left[\Delta p + \frac{b_m^2\rho_{l_m}\Delta\bar{V}^2}{2}\right.$$

$$\left. + \frac{b_m\rho_{l_m}\bar{V}_m^2}{1 + r_m}\left(\frac{s_m\Delta r}{1 + r_m} - \Delta s\right)\right] \qquad (29)$$

5. Heat Transfer

Although no heat is transferred to the mixture as a whole, heat transfer exists between the phases. Hence, a second energy equation must be written using as the control volume the boundary between the phases.

The work dW done on the liquid is that due to drag by the gas. (Only work done by shear or shaft forces is included in dW when writing the First Law for a control

volume). Multiplying Eq. (24) by the number flow rate of drops $\dot{N} = 6\dot{m}_L/\pi D^3\rho_L$, the drag force F_d on that quantity of liquid is

$$F_d = \frac{\dot{N}}{8}\rho_g |V_g| V_g C_D \pi D^2 = \frac{\dot{m}_l}{l}\frac{dp}{dx} + m_l V_l \frac{dV_l}{dx} \tag{30}$$

The work done on the liquid is

$$-dW = F_d dx = \dot{m}_l\left(\frac{dp}{\rho_l} + \frac{dV_l^2}{2}\right) \tag{31}$$

The heat dQ transferred from the liquid is made up of two parts: (1) the convective cooling due to the temperature difference between the liquid and gas and (2) the evaporative cooling due to the latent heat supplied to the liquid vaporized. The convective cooling is

$$-dQ_c = hA_d\dot{N}(T_l - T_g)dt \tag{32}$$

where h is the heat-transfer coefficient, $A_d = \pi D^2$ is the surface area of a drop, and $dt = dx/V_L$ is the time required to traverse dx. Thus,

$$-dZ_c = \frac{6h\dot{m}_l(T_g - T_l)dx}{D\rho_l V_l} \tag{33}$$

The evaporative cooling is

$$-dQ_v = L_a d\dot{m}_{a_g} + L_b d\dot{m}_{b_g} \tag{34}$$

The change in enthalpy of the liquid over the pressure increment dp is

$$dH = \dot{m}_l \left(c_l dT_l + \frac{dp}{\rho_l} + \frac{dV_l^2}{2} \right) \tag{35}$$

Substituting Eqs. (31), (33), (34), and (35) into the steady-flow energy equation dQ - dW = dH, the result is

$$\frac{6h\dot{m}_l \delta T dx}{D\rho_l V_l} - L_a d\dot{m}_{a_g} - L_b d\dot{m}_{b_g} = \dot{m}_l c_l dT_l \tag{36}$$

where $\delta T = T_g - T_L$.

Writing for a finite interval, the final form of the drop heat-transfer equation is

$$\Delta T_l = \frac{1}{c_{l_m}} \left[\frac{6h\delta_m T \Delta x}{D\rho_{l_m} V_{l_m}} - L_{a_m} \frac{\Delta \dot{m}_{a_g}}{\dot{m}_{l_m}} - L_{b_m} \frac{\Delta \dot{m}_{b_g}}{\dot{m}_{l_m}} \right] \tag{37}$$

Equations (1), (17), (23), (28) and (37) are the five equations that must be solved simultaneously to obtain the values of the five dependent variables D, T_g, T_L, V_g, and V_L as a function of the independent variable p. To carry out the solution all quantities in the equations must be expressed in terms of these six variables.

The preceding equations form the basis for the mathematical model which is used to predict, based on inlet conditions, the exit velocity, and temperature of the mixture. These equations also form the basis for the model which provides the optimum nozzle shape given a set of inlet

conditions. Some additional relationships are, however, required. These are:

1. Phase properties--to establish the mass ratio, mass flow rate ratio of gas to liquid, and the thermal conductivity of the mixture.
2. Liquid drop drag coefficients.
3. The liquid drop heat transfer coefficients.
4. Boundary layer momentum thickness and displacement thickness.
5. Skin friction coefficient.

These five additional relationships are developed in detail in Ref. 1.

The preceding "basic" model in conjunction with the additional equations form the core for four computer programs which provide real and isentropic flow output parameters, and an optimized nozzle contour given a set of inlet conditions.

Reference 1 reported that the optimum nozzle profile has an elongated throat region, that the required shape is insensitive to drop diameter and nozzle length, and that the exit velocity is insensitive to departures from the optimum shape. For given fluids and pressures, the exit velocity was found to be insensitive to nozzle length and flow rate beyond certain minimum values. This insensitivity of nozzle exit velocity to nozzle shape and size results from the inverse dependence of drop size on slip velocity, which

apparently acts to adjust the slip to a value that holds the exit velocity in the range 75 to 90% of isentropic. Thus, it is difficult to design either a very good or a very poor two-phase nozzle.

V. EXPERIMENTAL APPARATUS

The experimental apparatus was designed to provide a facility to study the performance of a Bi-phase nozzle. The basic requirements were to allow overall nozzle performance evaluation as well as optical diagnostic probing of the Bi-phase flow-field.

The experimental system can be conveniently grouped into five subsystems. These are: the nozzle proper, nozzle assembly, air supply system, liquid injection system, and nozzle exhaust plane instrumentation. Each subsystem is described in the following sections. Figure 8 is an overall system drawing.

A. NOZZLE

The nozzle was designed based on recommendations given in Refs. 1 and 5. It is convergent-divergent, 12 in. long with a throat area of 0.25 $in.^2$. Inlet area is 2.0 $in.^2$. The throat is located 4 in. from theinlet (1/3 of the overall length). The nozzle is constructed by "sandwiching" two ½ inch thick machined aluminum nozzle profile plates between ½ inch plexiglass plates (Figs. 9 and 10). The aluminum nozzle plates are located at the end of a 30 inch long "test" section and are easily replaceable. The test section provides the necessary space for pressure taps, liquid injection tubes, and other instrumentation and

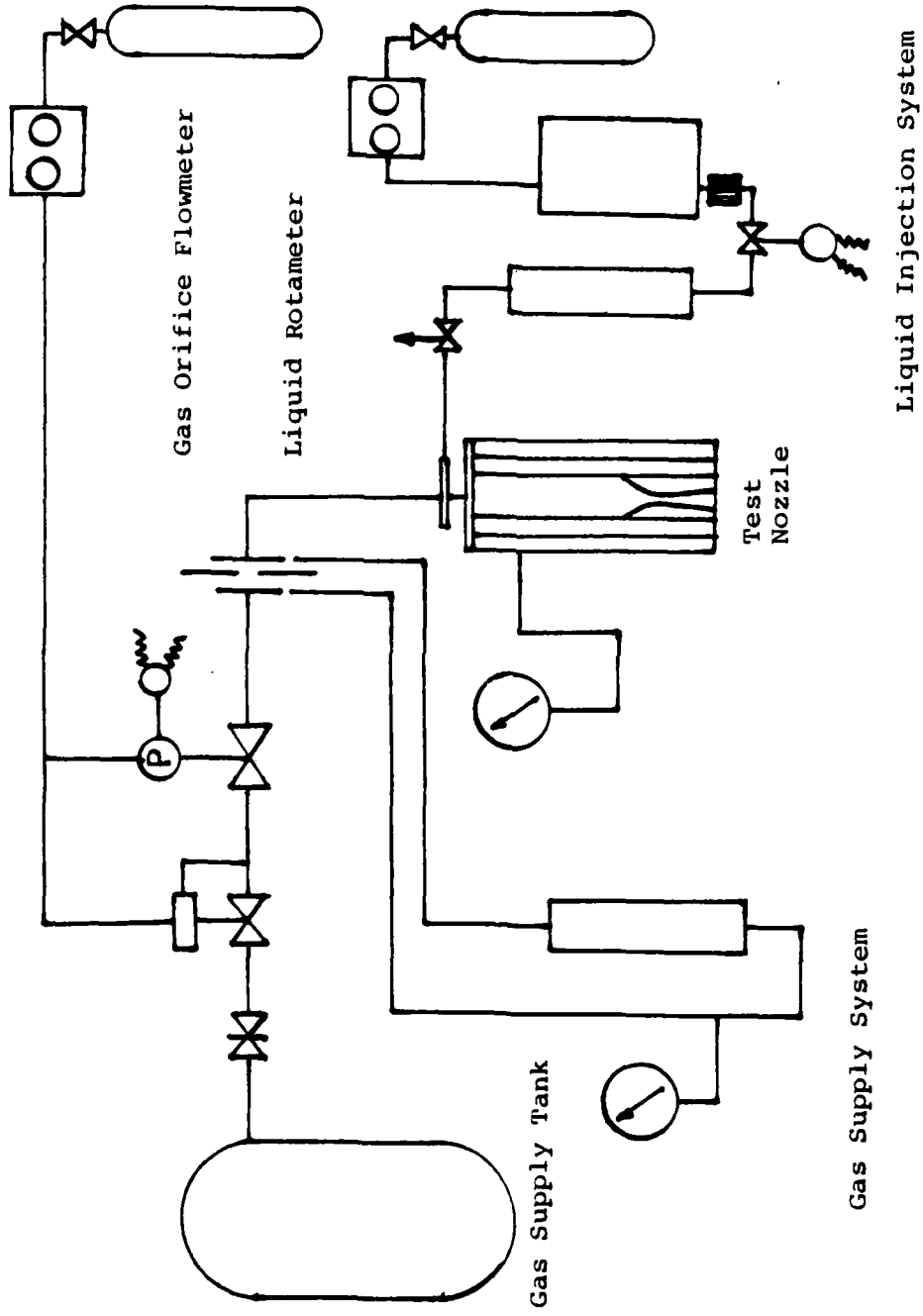

Fig. 8. Overall System Drawing

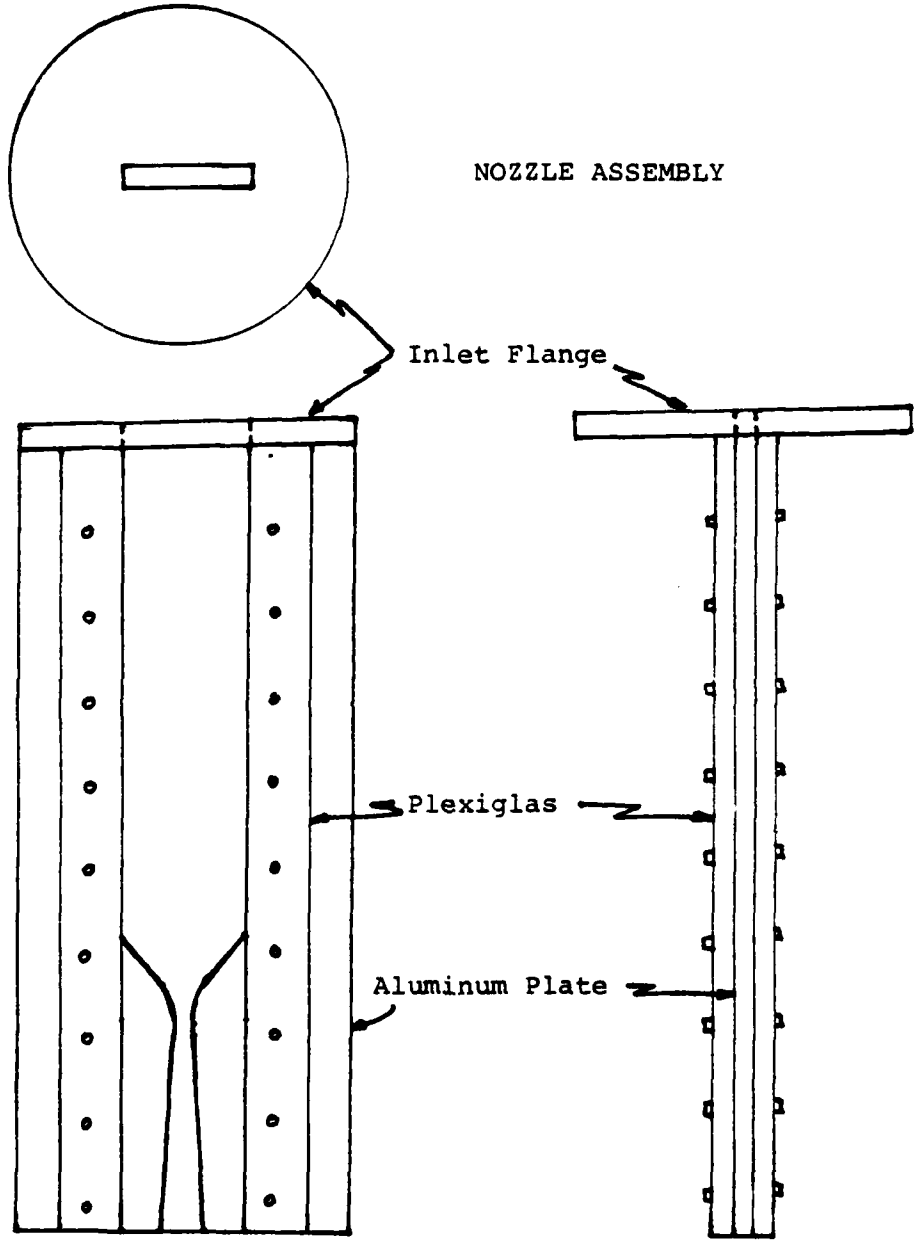

Fig. 9. Nozzle Assembly Drawing.

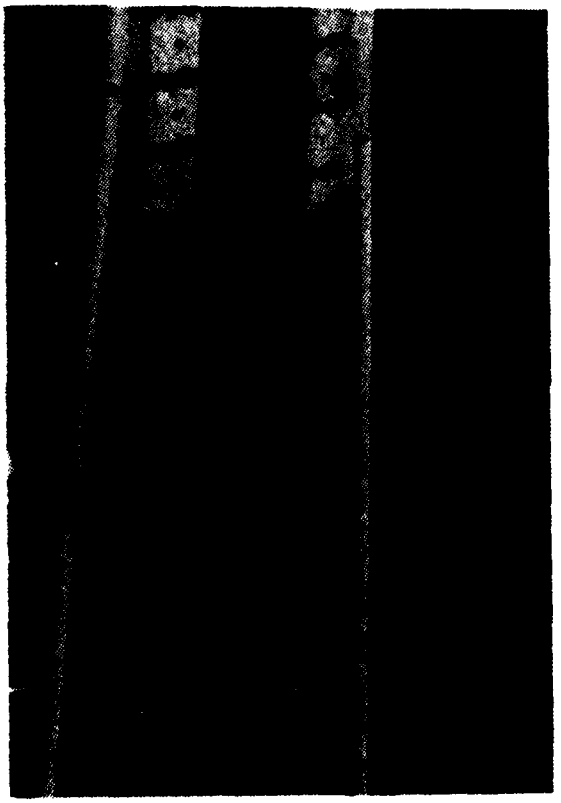

Fig. 10. Nozzle Assembly Photograph.

configuration options. The ability to replace the nozzle profile plates allows for modification of the nozzle configuration.

B. AIR SYSTEM (Fig. 11)

Two 117 ft.^{3} tanks supplied with compressed air from an Ingersol Rand three cylinder air compressor provide the air storage volume required to support nozzle operation. The nozzle is supplied with air at variable pressure via 3" ID piping. The air supply piping contains two pressure control valves, a solenoid actuated nitrogen operated 3 in. ball valve, and a flow measurement orifice plate. The orifice flow coefficient was determined from Ref. 6, Table 4. The air mass flow rate can be determined from the equation

$$W_h = 359\ K\ d^2 Fa\ Y\ \sqrt{h_w \gamma}$$

where

W_h - air mass flow rate in LBm/HR

K - orifice flow coefficient Table 4 [Ref. 6]

d - orifice diameter

F_a - thermal expansion factor Fig. 38 [Ref. 6]

y - expansion factor, Fig. 40b [Ref. 6]

h_w - differential pressure in H_2O at 68°F

γ - Specific weight of the flowing fluid at the inlet side of the primary element (LB/FT^3)

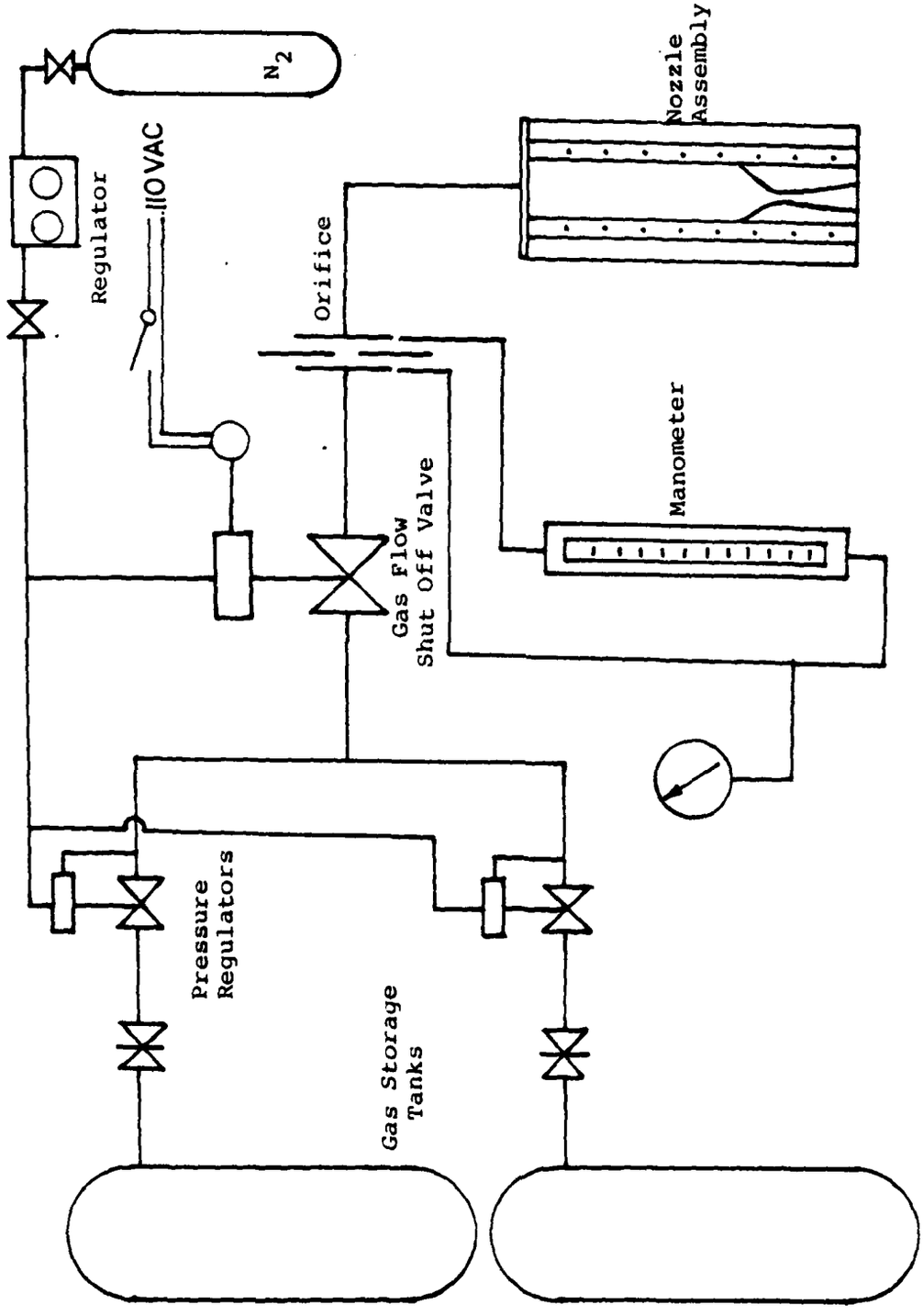

Fig. 11. Gas Flow Drawing.

and

$$h_w = \frac{h_m(\gamma_m - \gamma_o)}{62.317}$$

where

h_m - inches of differential of inches of manometer fluid

γ_m - specific weight of manometer fluid LB/FT^3

γ_o - specific weight of fluid separating manometer from flowing fluid

h_w - differential head, in. of H_20 at 68^oF

And

$$\gamma = \gamma_a$$

Where

γ_a = specific weight of dry air at actual temperature.

For an example calculation, see Appendix 2, example 5 from Ref. 6.

C. LIQUID INJECTION SYSTEM (Fig. 12)

The liquid injection system consists of a pressure vessel to contain the water which is pressurized from a nitrogen tank. The pressure vessel supplies pressurized water to the injection tube via a solenoid stop valve, a flow control valve and a flowmeter. The flowmeter was calibrated using an accurate scale and a stop watch. The calibration data and chart are recorded in Fig. 13. The liquid injector is a 0.25 in. brass tube inserted in

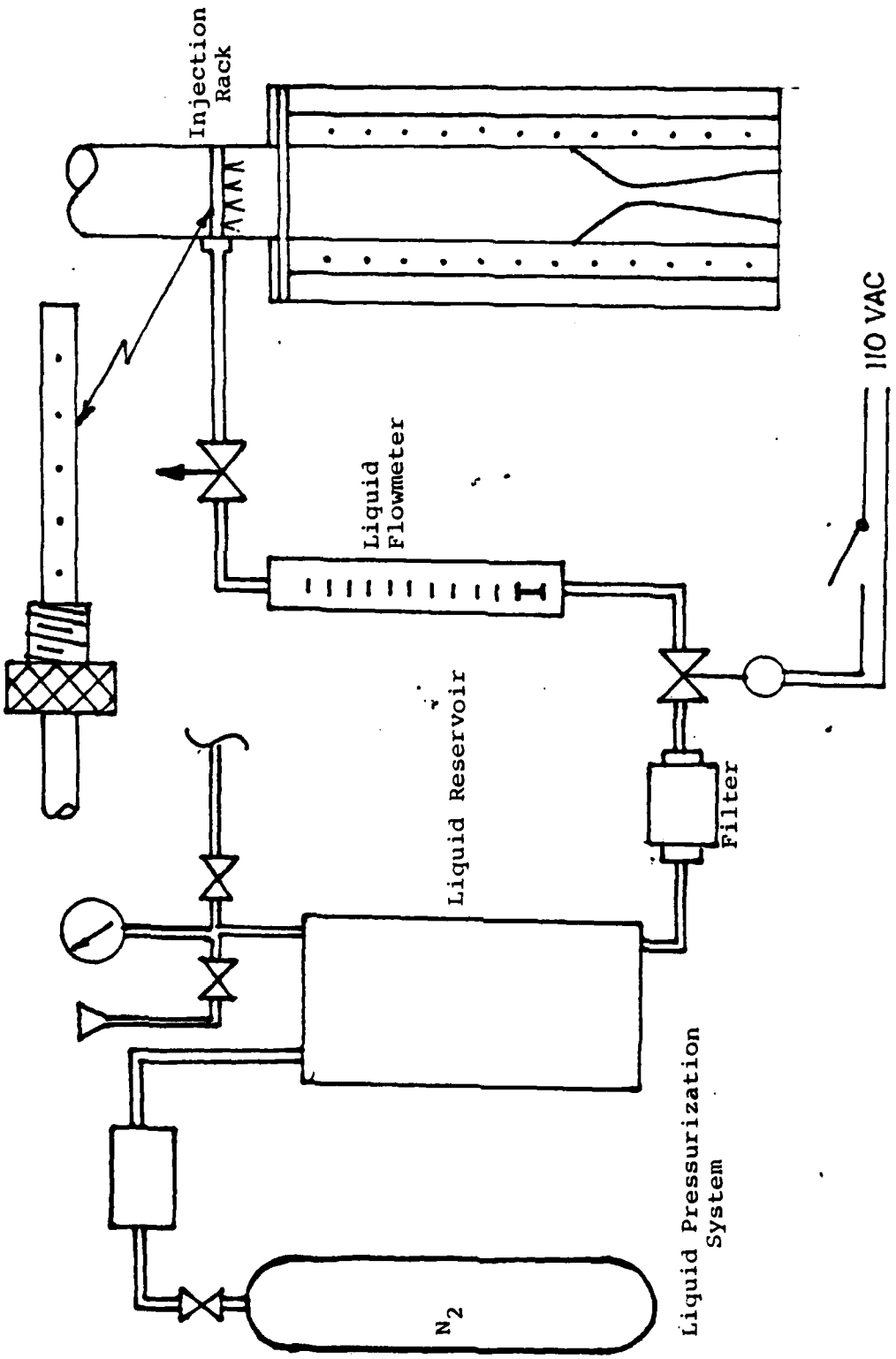

Fig. 12. Liquid Flow Drawing.

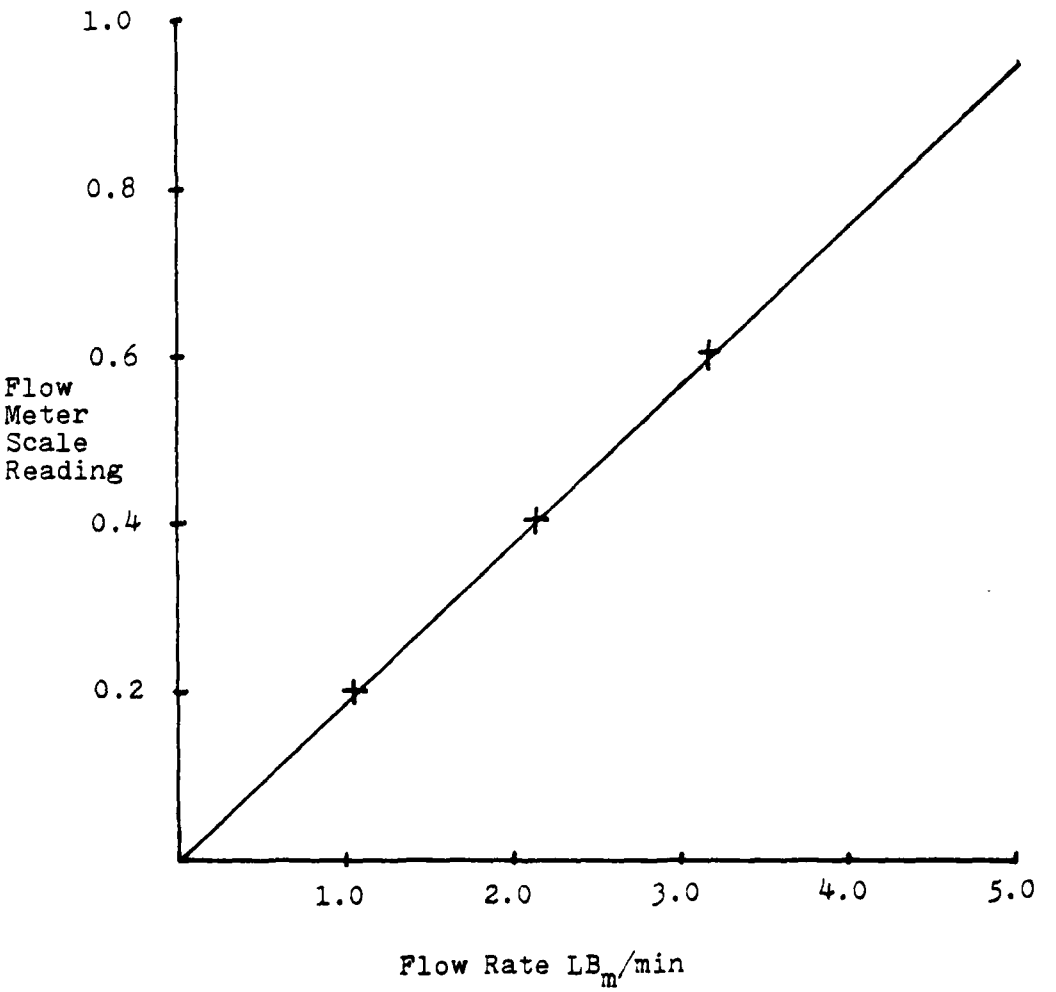

Fig. 13. Liquid Fl meter Calibration Curve.

the 3 in. ID air supply pipe just upstream of the flange connection to the test section. The injector tube is drilled with 5 holes facing the test section entrance. It has been proposed that more efficient liquid atomization could improve nozzle efficiency; therefore, the drilled holes were made as small as possible consistent with achieving a significant liquid mass flow rate.

D. NOZZLE EXHAUST INSTRUMENTATION

A cylindrical drag body, which is attached to a rectangular cantilever beam, is placed in the nozzle exhaust flow stream. The drag body unit is attached to a bracket which is attached to a rectangular transversing plate (Figs. 14 and 15). The transversing plate is screw driven to move in a transverse direction across the nozzle exhaust. This movement causes the cylinder to move through the entire nozzle exhaust flow stream. By placing strain gages on the drag body unit, the cantilever beam deflection can be determined and related to the force on the cylindrical portion of the drag body. That force, in turn, can be related to the local velocity of the flow stream and these velocities plotted to give a velocity distribution at the nozzle exhaust. A similar plot can be constructed for the momentum distribution

$$\text{Drag } (LB_f) = C_D \, A \, \frac{\rho U^2}{2}$$

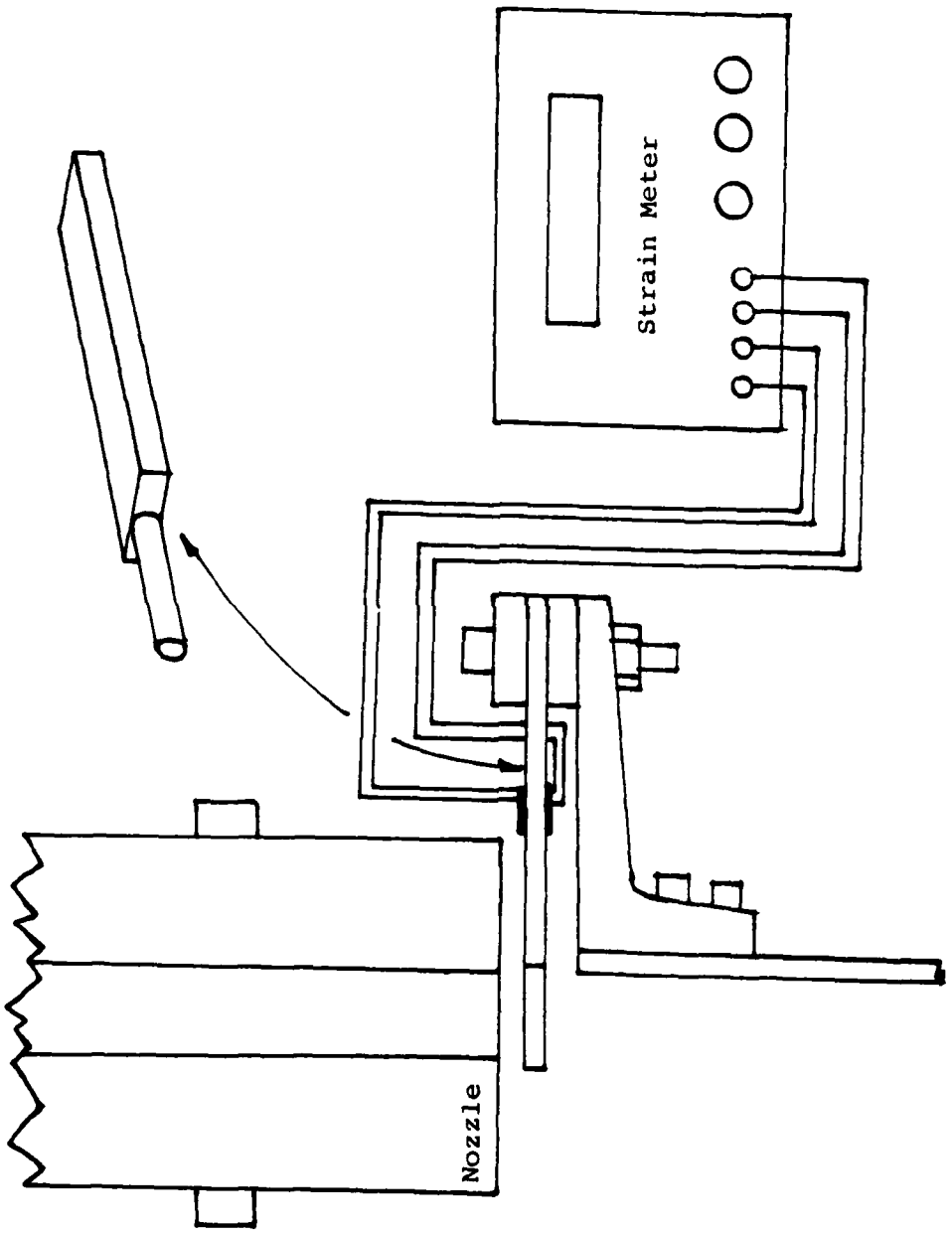

Fig. 14. Instrumentation Drawing.

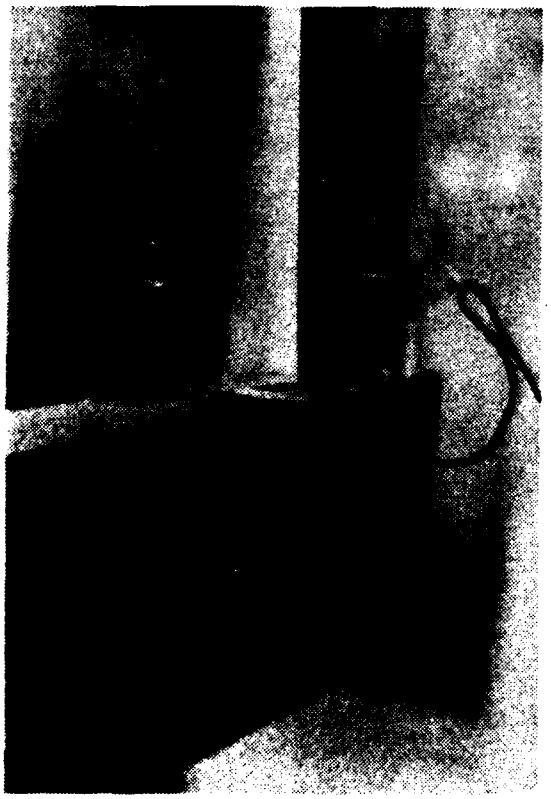

Fig. 15. Instrumentation Photograph.

where

C_D - Drag coefficient of the cylinder

- (Smooth cylinder 1/8 in. in diameter)

A - Projected area of the cylinder 1/2" X 1/8" = 1/16 $in.^2$

ρ - Density of the mixture

U - Local velocity of the exhaust flow stream

Solving for U:

$$U = \sqrt{\frac{2 \text{ X Drag force}}{\rho C_D A}}$$

Figures 16 and 17 are calibration data for the drag cylinder.

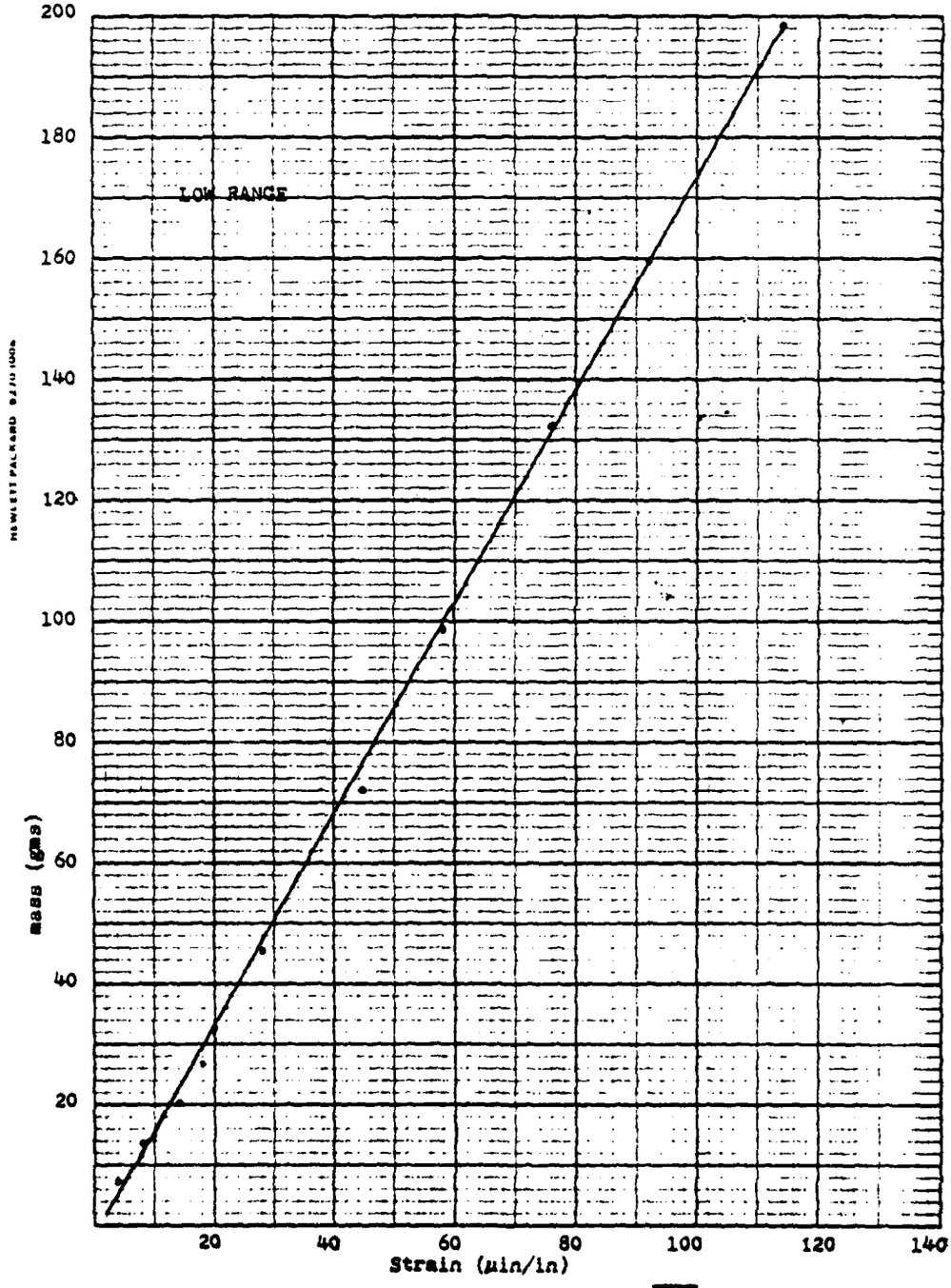

Fig. 16. Drag Cylinder Calibration Curve.

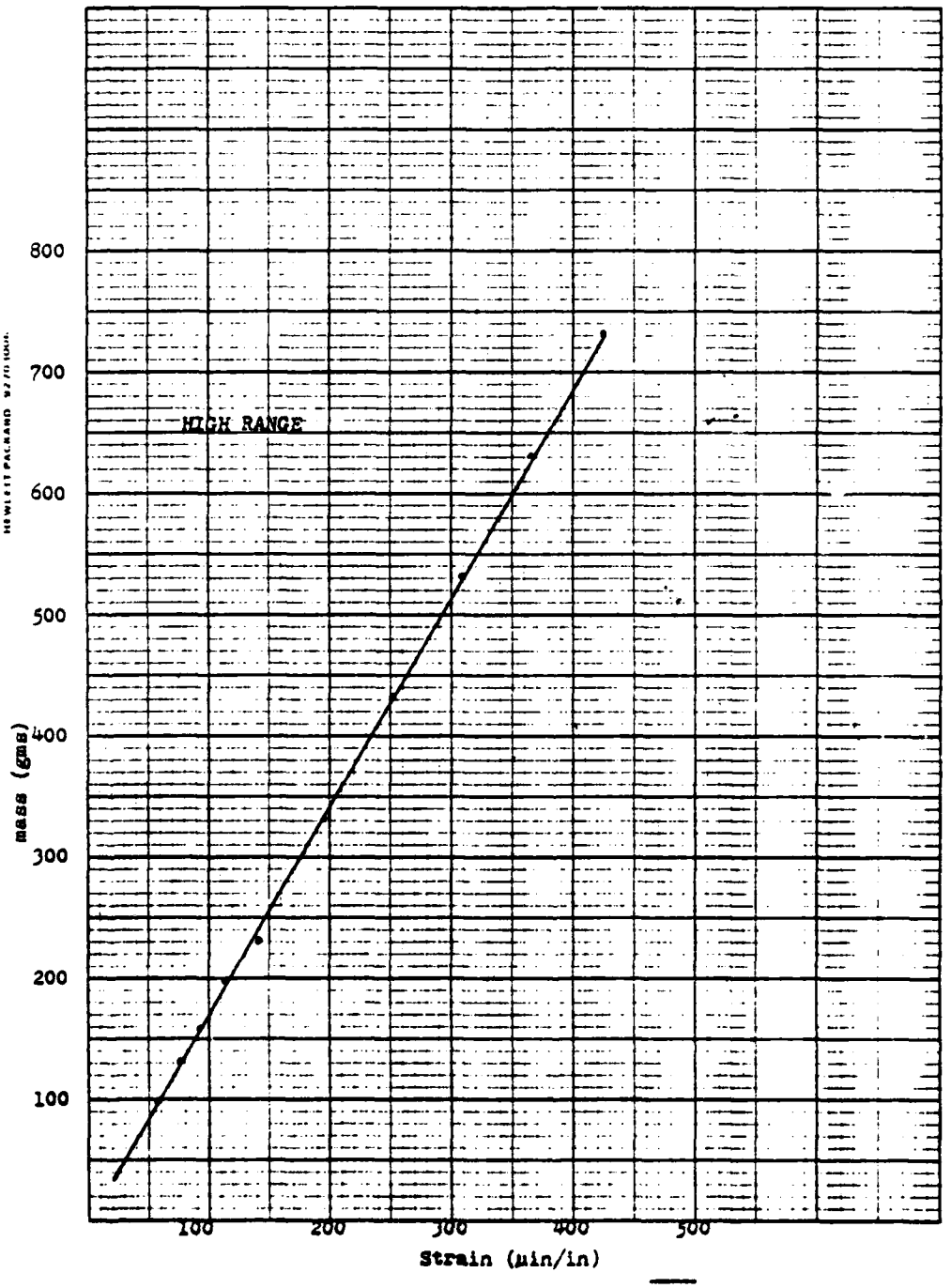

Fig. 17. Drag Cylinder Calibration Curve.

VI. CONCLUSIONS

Successful Bi-phase nozzle operation was achieved and sustained under controlled conditions. Liquid injection, nozzle, and instrumentation system all operate satisfactorily. The liquid breakup and acceleration in the nozzle passage was observed.

With the nozzle pressures employed, i.e., 20, 30, 40, and 50 psig an instability was observed in the downstream portion of the nozzle passage. It was apparent that, for the nozzle geometry installed, there was a transition from supersonic flow in the throat region to subsonic conditions in the diverging downstream passage. It is apparent that at this point the passage converts from a supersonic nozzle to a subsonic diffuser. The transition point appeared to be unsteady, initiating alternatively from the sides of the nozzle. The position at which transition takes place could be controlled at will. As the liquid mass ratio and/or upstream pressure were increased, the passage tended to perform as a supersonic nozzle, i.e., the supersonic-subsonic transition was driven further downstream towards the exit. This is as one would expect. As the liquid mass ratio is increased, the sonic velocity decreases and the passage tends to a supersonic nozzle. Also, as the pressure ratio increases, the shock or transition to subsonic

conditions is driven downstream. An exit plane survey (Fig. 18) using the instrumented drag cylinder confirms the existance of a transition point somewhere in the diverging portion of the flow passage. Thus, one is led to conclude that the role of change of flow passage area is too high for the test pressure ratios. From Fig. 18 it is also evident that the flow tended to oscillate from one side of the nozzle to the other. This was confirmed by visual observations as well as audible pulsations.

It would be desirable to develop a degree of flexibility in changing or altering the nozzle profiles, particularly the diverging passage. Originally it was envisioned to replace the nozzle inserts; however, it may be more expeditious to provide an infinitely and continuously variable system. This may be achieved by a flexure system controlled by jack screws in the exit plane. The second desirable aspect would be the capability to diagnostically probe the flow field in the passage proper. A laser anemometer may provide the capability; however, no information exists on the use of LDA in Bi-phase flow.

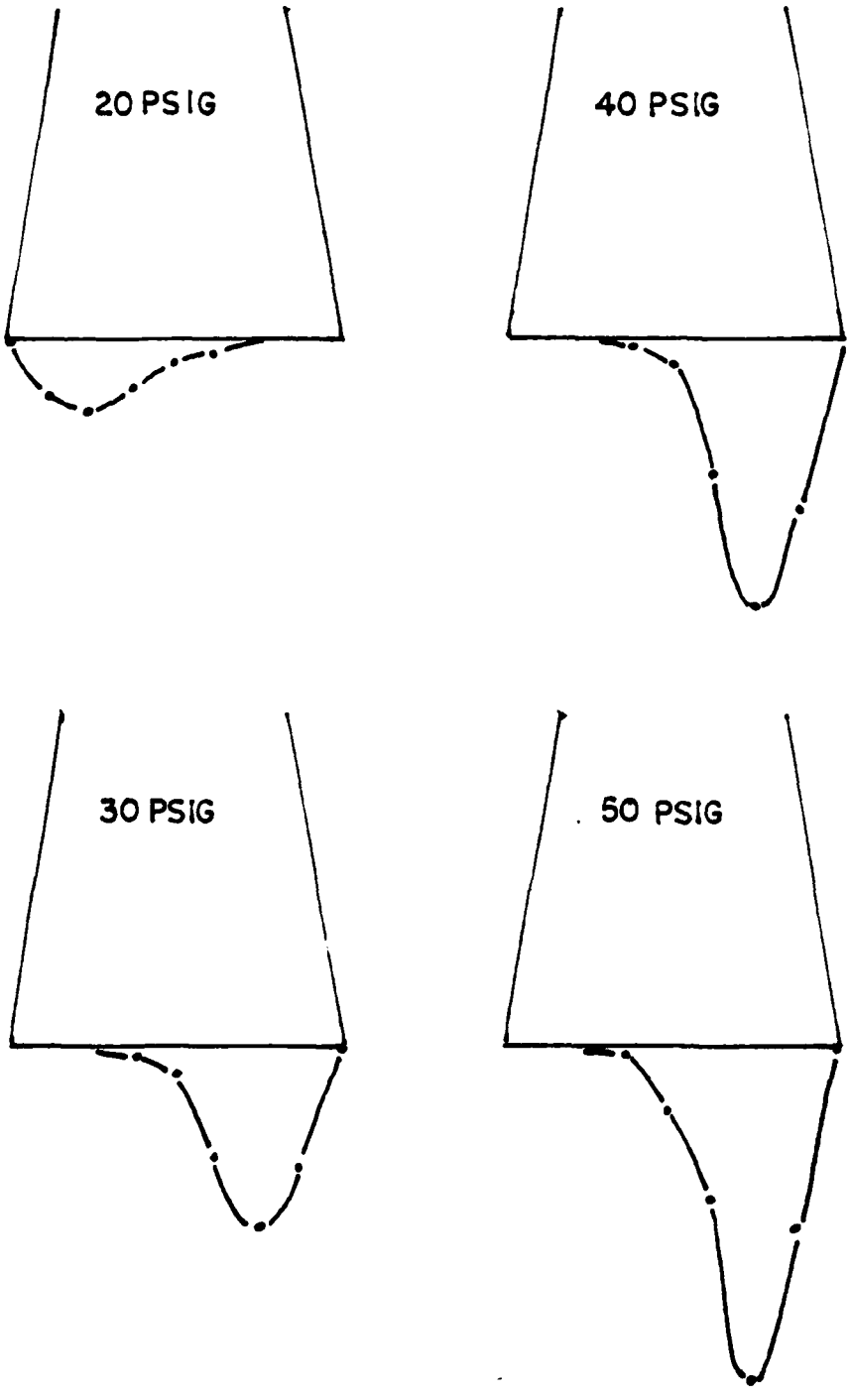

Fig. 18. Nozzle Exit Force Distributions.

LIST OF REFERENCES

1. National Aeronautics and Space Administration, Technical Report 32-987, Acceleration of Liquids in Two-Phase Nozzles by D. G. Elliott and E. Weinberg, July 1968.

2. Biphase Energy Systems Subsidiary of Research - Cottrell, Inc., Report No. 106-F, Design Study of a Two-Phase Turbine Engine for Submarine Propulsion by E. Ritzi and L. Hays, July 1977.

3. AIAA/SAE/ASME 17th Joint Propulsion Conference, Report AIAA-81-1604, Biphase Turbine for Marine Propulsion by L. Hays, July 1981.

4. Olson, R. M., Essentials of Engineering Fluid Mechanics, 4th Ed., Harper & Row, 1980.

5. The Office of Naval Research Report R81-977229-4, Two Phase Nozzle Theory and Parametric Analysis by C. W. Deane and S. C. Kuo, July 1981.

6. Flow Measurement/Instruments and Apparatus, Part 5 - Measurement of Quantity of Materials, The American Society of Mechanical Engineers, February 1959.

BIBLIOGRAPHY

Berstein, A., Heiser, W., H. and Hevenor, C., Compound-Compressible Nozzle Flow, Journal of Applied Mechanics Paper No. 67-APM-L, November 1966.

Cerini, D. J., A Two-Phase Rotary Separator Demonstration System for Geothermal Energy Conversion, 12th IECEC Paper No. 770135.

Cerini, D. J. and Hays, L. G., Power Production from Geothermal Brine with the Rotary Separator Turbine, American Institute of Aeronautics and Astronautics, Inc., Paper No. 809156, 1980.

Colwell, G. T., Low Density Nozzle Flow, The American Society of Mechanical Engineers Paper No. 68-WA/FE-9, August 1968.

Dash, S. M. and Thorpe, R. D., Shock-Capturing Model for One and Two-Phase Supersonic Exhaust Flow, American Institute of Aeronautics and Astronautics Paper No. 80-1254, February 1981.

Ganic, E. M. and Rohsenow, W. M., On the Mechanism of Liquid Drop Deposition in Two-Phase Flow, The American Society of Mechanical Engineers Paper No. 76-WA/HT-18, July 1976.

Hays, L. and Neal, J., Biphase Turbines for Diesel Bottoming, Energy Research and Development Administration Paper No. 779077.

Hiley, P. E. and Wallace, H. W. and Booz, E. E., Nonaxisymmetric Nozzles Installed in Advanced Fighter Aircraft, AIAA/SAE 11th Propulsion Conference Paper No. 75-1316, August 1973.

Keenan, J. H. and Kaye, J., Gas Tables, John Wiley & Sons, Inc. 1948.

Lewis, W. G. E., Propelling Nozzle Research, Lecture given to the Society on April 23, 1963.

Li, W. and Lam, S., Principles of Fluid Mechanics, Addison-Wesley Publishing Co., 1964.

Muench, R. K., and Ford, A. E., A Water-Augmented Air Jet for the Propulsion of High-Speed Marine Vehicles, Paper presented at the AIAA 2nd Advanced Marine Vehicles and Propulsion Meeting, Seattle, Washington, May 1969.

Nunn, R. H., and Brandt, H., Aerodynamic Throttling of Two-Dimensional Nozzle Flows, August 1970

Replogle, J. A., Myers, L. E., and Brust, K., Flow Measurements with Fluorescent Tracers, March 1968.

Schlichting, H., Boundary-Layer Theory, McGraw-Hill Book Co., 1979.

Shapiro, A. E., The Dynamics and Thermodynamics of Compressible Fluid Flow, Vol. 1, The Ronald Press Co., 1953.

Streeter, V. L. and Wylie, E. B., Fluid Mechanics, Seventh Ed., McGraw-Hill Book Co., 1979.

Thornock, R. L. and Brown, E. F., An Experimental Study of Compressible Flow Through Convergent-Conical Nozzles, Including a Comparison with Theoretical Results, ASME Publication Paper No. 71-WA/FE-3, June 1971.

Wagner, J. L., A Cold Flow Field Experimental Study Associated with a Two-Dimensional Multiple Nozzle, 1971.

Wagner, W. B., and Owczarek, J. A., An Investigation of the Corner Secondary Flows Generated in Planar Nozzles, The American Society of Mechanical Engineers Paper No. 73-WA/Fles-5, August 1973.

The American Society of Mechanical Engineers Paper No. 80-GT-90, Some Effects of Using Water as a Test Fluid in Fuel Nozzle Spray Analysis, December 1979.

Air Force Systems Command Report SRD-73-161, Techniques for Injection and Acceleration of Particles by Ultra High Speed Gas Jets, February 1974.

INITIAL DISTRIBUTION LIST

		No. Copies
1.	Defense Technical Information Center Cameron Station Alexandria, Virginia 22314	2
2.	Library, Code 0142 Naval Postgraduate School Monterey, California 93940	2
3.	Department Chairman, Code 69 Department of Mechanical Engineering Naval Postgraduate School Monterey, California 93940	1
4.	Professor Joseph Sladky, Code 69Zy Department of Mechanical Engineering Naval Postgraduate School Monterey, California 93940	3
5.	LCDR Michael E. Flenniken USS THOMAS JEFFERSON (SSN 618) FPO New York 09575	1

END

DATE
FILMED

3-82

DTIC